Molecular Plant • Volume 3 • Number 1 • Pages 156–173 • January 2010 RESEARCH ARTICLE

Mild Reductions in Mitochondrial NAD-Dependent Isocitrate Dehydrogenase Activity Result in Altered Nitrate Assimilation and Pigmentation But Do Not Impact Growth

Agata Sienkiewicz-Porzucek[a,2], Ronan Sulpice[a,2], Sonia Osorio[a], Ina Krahnert[a], Andrea Leisse[a], Ewa Urbanczyk-Wochniak[a], Michael Hodges[b], Alisdair R. Fernie[a,1] and **Adriano Nunes-Nesi[a]**

a Max-Planck-Institut für Molekulare Pflanzenphysiologie, 14476 Potsdam-Golm, Germany
b Institute de Biotechnologie des Plantes, Unité Mixte de Recherche 8618, Centre National de la Recherche Scientifique, Université de Paris-Sud 11, 91405 Orsay Cedex, France

ABSTRACT Transgenic tomato (*Solanum lycopersicum*) plants were generated expressing a fragment of the mitochondrial NAD-dependent isocitrate dehydrogenase gene (*Sl*IDH1) in the antisense orientation. The transgenic plants displayed a mild reduction in the activity of the target enzyme in the leaves but essentially no visible alteration in growth from the wild-type. Fruit size and yield were, however, reduced. These plants were characterized by relatively few changes in photosynthetic parameters, but they displayed a minor decrease in maximum photosynthetic efficiency (Fv/Fm). Furthermore, a clear reduction in flux through the tricarboxylic acid (TCA) cycle was observed in the transformants. Additionally, biochemical analyses revealed that the transgenic lines exhibited considerably altered metabolism, being characterized by slight decreases in the levels of amino acids, intermediates of the TCA cycle, photosynthetic pigments, starch, and NAD(P)H levels, but increased levels of nitrate and protein. Results from these studies show that even small changes in mitochondrial NAD-dependent isocitrate dehydrogenase activity lead to noticeable alterations in nitrate assimilation and suggest the presence of different strategies by which metabolism is reprogrammed to compensate for this deficiency.

Key words: Carbon metabolism; nitrogen metabolism; photorespiration; photosynthesis; mitochondria; tomato.

INTRODUCTION

Studies surveying metabolic changes of plants exposed to environmental or genetic perturbations have indicated an important role for 2-oxoglutarate (2OG) within ammonium assimilation (Hodges, 2002; Hodges et al., 2003; Dutilleul et al., 2005; Fritz et al., 2006; Schneidereit et al., 2006). It has been proposed that this 2OG is either synthesized in the mitochondrial matrix by NAD-dependent isocitrate dehydrogenase (IDH), which catalyzes a tricarboxylic acid (TCA) cycle reaction wherein isocitrate is oxidized and decarboxylated to yield 2OG, NADH, and CO_2 (Siedow and Day, 2000), or in the cytosol, by NADP-dependent isocitrate dehydrogenase (ICDH; Chen, 1998).

NAD-dependent IDH is located exclusively in the mitochondrial matrix, whereas the NADP-dependent isoforms are found in several organelles, such as the chloroplasts (Gálvez et al., 1994), mitochondria (Gálvez et al., 1998), peroxisomes (Corpas et al., 1999), and in the cytosol (Gálvez et al., 1996). NADP-dependent mitochondrial ICDH is a homodimeric enzyme that is likely to have highest activity *in vivo* (Møller and Rasmusson, 1998). Study in mammals' cells indicates that it plays a key role in cellular defense against oxidative stress-induced damage (Jo et al., 2001). Likewise, in plants, recently, the physiological role for mitochondrial NADP-dependent ICDH has been investigated and this study suggests this enzyme as a regulatory

[1] To whom correspondence should be addressed. E-mail fernie@mpimp-golm.mpg.de, fax +49 (0)331 5678408, tel. +49 (0)331 5678211.

[2] These authors contributed equally to the work.

doi: 10.1093/mp/ssp101, Advance Access publication 24 December 2009
Received 15 June 2009; accepted 30 October 2009

switch involved in TCA cycle flux and modulation of alternative oxidase (Gray et al., 2004). Expression of a tobacco cDNA encoding NAD-dependent IDH in a yeast complementation study suggests that the plant NAD-dependent IDH enzyme is composed of three different subunits, one being catalytic and two regulatory subunits (Lancien et al., 1998). In *Arabidopsis*, five IDH genes have been identified, two genes encoding catalytic subunits and three regulatory subunits (Lemaitre and Hodges, 2006). The number of IDH encoding genes varies from three in rice (Abiko et al., 2005) and tobacco (Lancien et al., 1998) to six (five transcribed and one pseudogene) in *Arabidopsis* (Lemaitre and Hodges, 2006). Although four genes of the latter were expressed in all plant organs and only one exhibited tissue-specific pollen expression, the transcription level of IDH genes differs between tissues, presumably reflecting the specific function of different isoforms (Lemaitre and Hodges, 2006). Despite the fact that multiple isoforms of isocitrate dehydrogenase have been postulated to be engaged in the production of carbon skeletons and reducing equivalents for multiple biosynthetic reactions in various cellular compartments, evidence of their exact physiological roles are currently somewhat limited. Amongst all NADP-requiring ICDH isoforms, the cytosolic one has the highest activity (Gallardo et al., 1995; Gálvez et al., 1996; Palomo et al., 1998). It has been intensively studied and, as such, is well characterized in plants. It accounts for 95% of total NADP–ICDH activity in green tobacco leaf tissue (Gálvez et al., 1996) and seems to be the predominant isoform in leaves of at least 15 plant species (Chen, 1998). Similarly, although the potato NADP–ICDH gene was active in all plant organs, its expression was highest in green tissues, flowers, and roots (Fieuw et al., 1995). Due to the preferential expression of this isoform in mature leaf veins, the enzyme has been postulated to be involved in cycling, redistribution, and export of amino acids, in addition to its primary function in GS/GOGAT-dependent nitrogen assimilation. The latter role was initially proposed by Chen and Gadal (1990) as a part of a cytosol-localized pathway producing carbon skeletons for ammonium assimilation in circumstances in which TCA cycle activity is decreased. It was, therefore, surprising to find that both transgenic potato (Kruse et al., 1998) and tobacco (Gálvez et al., 1999) antisense plants displaying only 6–10% residual ICDH activity showed neither growth nor developmental phenotypes. Considerable research effort has been expended in an attempt to elucidate the metabolic and physiological functions of the various isoforms of isocitrate dehydrogenase (Lemaitre et al., 2007; Hodges et al., 2003; Gálvez et al., 1994). In light of the strategic positional importance of this enzyme, studies investigating its metabolic importance in plants surprisingly remain limited (Scheible et al., 2000; Bläsing et al., 2005; Urbanczyk-Wochniak et al., 2005).

As part of our ongoing project to determine the function of the TCA cycle in illuminated leaves, we have, thus far, characterized the *Aco*1 *Solanum pennellii* mutant deficient in aconitase expression (Carrari et al., 2003), as well as transgenics of cultivated tomato deficient in the expression of the mitochondrial isoforms of malate dehydrogenase (Nunes-Nesi et al., 2005), fumarase (Nunes-Nesi et al., 2007), succinyl–CoA ligase (Studart-Guimarães et al., 2007), and citrate synthase (Sienkiewicz-Porzucek et al., 2008). These genetic studies have generally corroborated those based on the use of mitochondrial inhibitors (for review, see Raghavendra and Padmasree, 2003; Sweetlove et al., 2007) in demonstrating a role for the mitochondria in optimizing photosynthesis. Furthermore, they agree with results from the analysis of plant genotypes directly affected in activities of proteins associated with normal functioning of the mitochondrial electron transport chain (see, e.g. Strodtkötter et al., 2009; Garmier et al., 2008; Bartoli et al., 2005; Dutilleul et al., 2003). It is, however, worth noting that the characterization of genetic perturbations of the TCA cycle has revealed mixed results when addressed from the perspective of cellular metabolism in general. Intriguingly, the manipulation of aconitase, fumarase, and mitochondrial malate dehydrogenase activities appeared to have far greater consequence than that of the mitochondrial reactions catalyzed by succinyl–CoA ligase, and citrate synthase (Nunes-Nesi et al., 2005, 2007; Studart-Guimarães et al., 2007; Sienkiewicz-Porzucek et al., 2008). The former three manipulations displayed clear effects on the rate of both photosynthesis and respiration at least under optimal growth conditions (Carrari et al., 2003; Nunes-Nesi et al., 2005, 2007, 2008), whereas the later two displayed no obvious physiological effects under similar conditions (Studart-Guimarães et al., 2007; Sienkiewicz-Porzucek et al., 2008). However, the effect of modifying respiration was considerably less when compared to the roots of the mMDH and fumarase lines (van der Merwe et al., 2009), or in potato tuber material in which the activity of the 2-oxoglutarate dehydrogenase complex (2OGDH) had been chemically inhibited (Araújo et al., 2008). In this study, we turn our attention to the evaluation of the importance of mitochondrial isocitrate dehydrogenase for metabolism in the illuminated tomato leaf. We describe here the generation of tomato transgenic plants exhibiting mild decreases in the expression of the mitochondrial NAD-dependent isocitrate dehydrogenase (mIDH). The transgenic lines generated were comprehensively characterized at transcriptional, biochemical, and physiological levels. The present results are discussed in the context of current models concerning the importance of the TCA cycle and of the coordination of plant carbon and nitrogen metabolism in the illuminated leaf.

RESULTS

Analysis of Mitochondrial and Cytosolic Isocitrate Dehydrogenases from Tomato

Searching tomato EST collections (Van der Hoeven et al., 2003) revealed the presence of seven tentative consensus sequences (TC193092; TC164449; TC196623; TC198615; TC201555; TC202045; TC216549) encoding isocitrate dehydrogenase, with only three TCs having above 90% identity to the

previously annotated isocitrate dehydrogenases from other species (TC193092, TC164449, and TC202045). The phylogenetic tree of plant isocitrate dehydrogenases displays two clear clusters, one in which TC164449 and TC202045 groups with NADP-specific isoforms and a TC193092 cluster with mitochondrial NAD-specific isoforms (Figure 1A). Assembly and sequence analysis of TC164449 revealed an open reading frame of 415 amino acids with high homologies to NADP-dependent ICDH (*Sl*ICDH2). Comparison with functionally characterized NADP isocitrate dehydrogenases revealed 91% identity to tobacco (*Nicotiana tabacum*, P50218, X77944) and 90% identity to potato (*Solanum tuberosum*,

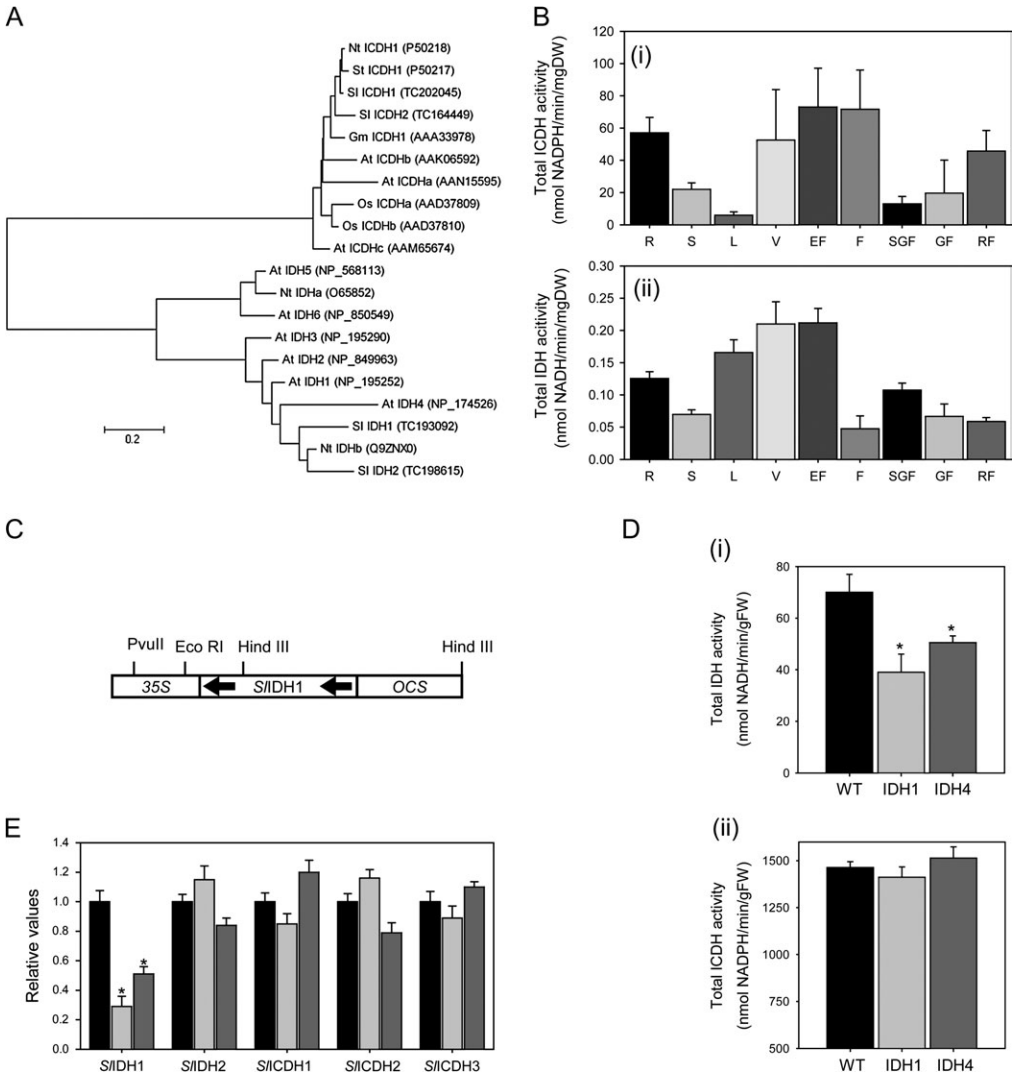

Figure 1. Characterization and Expression of Tomato Mitochondrial Isocitrate Dehydrogenase (*Sl*IDH).

(A) Dendogram of *Sl*IDH and *Sl*ICDH amino acid sequences. The protein accession numbers are given between brackets.

(B) Total ICDH (i) and IDH (ii) activity in different organs of 9-week-old tomato plants. Values are presented as means ± SE of three individual plants.

(C) Construction of a chimeric gene for the expression of tomato *Sl*IDH1 antisense consisting of a 514-bp fragment encoding the CaMV 35S promoter and a 734-bp (antisense) for *Sl*IDH1 and the 200-bp *ocs* terminator.

(D) Total IDH (i) and ICDH (ii) activities determined in 5-week-old leaves taken from fully expanded source leaves of transgenic plants with altered expression of *Sl*IDH1 as compared to wild-type.

(E) Relative transcript abundance of the various cellular isoforms of isocitrate dehydrogenase. The abundance of isocitrate dehydrogenase mRNAs was measured by quantitative RT–PCR. Values are presented as mean ± SE (n = 5). An asterisk indicates significantly different ($P < 0.05$) values obtained for each line in comparison to wild-type as determined by the t-test. *Sl*IDH1 (TC193092), *Sl*ICDH1 (TC202045); *Sl*ICDH3 mitochondrial ICDH-like protein (TC196623); *Sl*ICDH2 (TC164449); *Sl*IDH2 (TC198615). The lines used were: wild-type, black bars; IDH1, light-gray bars; IDH4, gray bars. Nt, *Nicotiana tabacum*; St, *Solanum tuberosum*; Sl, *Solanum lycopersicum*; Gm, *Glycine max*; At, *Arabidopsis thaliana*; Os, *Oryza sativa*; R, roots; S, stems; L, fully expanded leaves; V, veins; EF, epidermal fragments; F, flowers; SGF, 3–6 days after pollination (DAP) fruits; GF, green fruits (~35 DAP); RF, red fruits (~60 DAP).

CAA53300, X75638). The sequence analysis of TC202045 also revealed an open reading frame of 415 amino acids with high homologies to NADP-dependent ICDH (*Sl*ICDH1). Comparison of this isoform to functionally characterized NADP-dependent isocitrate dehydrogenases revealed 96% identity to tobacco (*Nicotiana tabacum*, P50218, X77944) and 98% identity to potato (*Solanum tuberosum*, P50217, X75638). The same procedure was adopted for TC193092, where a sequence analysis revealed an open reading frame of 393 amino acids with high homologies to NAD-dependent IDH (*Sl*IDH1). Comparison of this isoform to the functionally characterized NAD-dependent isocitrate dehydrogenases revealed 75% identity to tobacco (*Nicotiana tabacum*, CAA74776, Y14431) and 66% identity to IDH1 in *Arabidopsis* (*Arabidopsis thaliana*, NP_195252, At4g35260). *In silico* predictions indicate that *Sl*IDH1 bears characteristics of a mitochondrial transit peptide sequence, indicating a mitochondrial location, whereas *Sl*ICDH1 and 2 have a cytosolic location (data not shown).

IDH and ICDH Activity in Various Organs of Tomato

Several organs of greenhouse-grown tomato plants were analyzed with respect to IDH and ICDH activity. As seen in Figure 1B, when we compared the mitochondrial NAD-dependent activity (IDH) with the NADP-dependent isocitrate dehadrogenase (ICDH) activity, ICDH have higher levels in all tissues studied. When comparing the ICDH activity in different organs, ICDH has relatively higher activity levels in roots, veins, epidermal fragments, and flowers, whereas lowest ICDH activities were found in stems and leaves. Interestingly, ICDH activity changes with fruit development, increasing from 5 days after pollination (DAP) to 60 DAP fruits (Figure 1B, section i). When we assayed IDH activity using the same protein extracts, leaves, veins, epidermal fragments, and roots had highest IDH activity in comparison with stems, flowers, and tomato fruits. In contrast to ICDH, IDH activity decreases along with fruit development (Figure 1B, section ii).

Transgenic NAD-Dependent IDH Plants Showed No Change in Time of Flowering and Growth Rate

A 734-bp fragment of the tomato gene encoding *Sl*IDH1 was cloned in antisense orientation into the transformation vector pK2WG7 (Karimi et al., 2002; Figure 1C). The gene fragment was inserted between the cauliflower mosaic virus (CaMV) 35S promoter and the octopine synthase (*ocs*) terminator. Following *Agrobacterium tumefaciens*-mediated transformation, we transferred 67 IDH1 transformed tomato plants to the greenhouse. A screening of the lines was performed by a combination of total cellular IDH activity and Northern blot analyses (data not shown). These preliminary studies allowed the identification of two lines that showed a statistically significant and specific reduction in IDH1 expression and total IDH activity in leaves. These two transgenic lines were clonally propagated and transferred to the greenhouse alongside wild-type controls. Following a period of 5 weeks growth, leaves were harvested in the middle of the light period, and total IDH and ICDH activities were measured in order to confirm the reduced activity of IDH (Figure 1D, subsection i) and its effects on total ICDH activity (Figure 1D, subsection ii). To verify the specificity of the constructs as well as to ensure that no compensatory effect occurred in the expression of the other isoforms, a secondary screen was performed at the mRNA level, using an established quantitative RT–PCR protocol (Czechowski et al., 2004). This revealed that only *Sl*IDH1 expression was significantly reduced in the transgenic lines. Moreover, the expression of non-targeted isoforms was unaltered in the transformants (Figure 1E). When taken together, the combined evidence presented demonstrates that these two lines (IDH1 and IDH4) were suitable for assessing the effects of a mild reduction of the mitochondrial IDH isoform activity.

For phenotypic characterization, we grew the transgenic plants in the greenhouse side by side with wild-type controls. After 5 weeks growth, no clear difference could be observed in the growth of aerial parts of the plant (Figure 2A). Close inspection of the transformants revealed only a minor decrease in root dry mass (Figure 2B) and no consistent changes in stem (Figure 2C) and leaf (Figure 2D) biomass. From these results, it follows that the transformants displayed a relatively unaltered total biomass accumulation (Figure 2E). Given that antisense inhibition of citrate synthase led to inhibition of flower formation in potato plants (Landschütze et al., 1995) and changes in fruit yield were observed in several tomato genotypes deficient in TCA cycle enzymes (Carrari et al., 2003; Nunes-Nesi et al., 2005, 2007; Studart-Guimarães et al., 2007), we next evaluated flower and fruit production in the transgenic lines. For this purpose, we grew the transgenics until full maturity, counting daily the number of flowers produced. This study showed that the flowering time was not affected by the reduction in mitochondrial IDH as well as the total number of flowers produced by the transgenic and wild-type plants (Figure 2F). This observation reflected in an unaltered number of fruits produced (Figure 2G). However, the diameter of fruits was significantly reduced in both lines (Figure 2H), as was the total fresh fruit weight (Figure 2I).

Reduction of Mitochondrial IDH Activity Has Little Effect on the Relative Electron Transport or Assimilation Rates and a Minor Reduction in the Maximum Efficiency of PSII

Given that we use the constitutive CaMV 35S promoter in this study, we are unable to distinguish whether the changes observed in fruits were the consequence of effects in the fruit themselves or merely reflect changes in the source leaves. We, therefore, concentrate the current investigation on leaf metabolism. In addition to that, we have previously reported alterations in photosynthetic performance in tomato genotypes displaying reduced activity of aconitase (Carrari et al., 2003), mitochondrial malate dehydrogenase (Nunes-Nesi et al., 2005), and fumarase (Nunes-Nesi et al., 2007), as well as altered dark respiration in genotypes deficient in citrate synthase (Sienkiewicz-Porzucek et al., 2008). Given this, we next analyzed whether the IDH transformants exhibited alterations

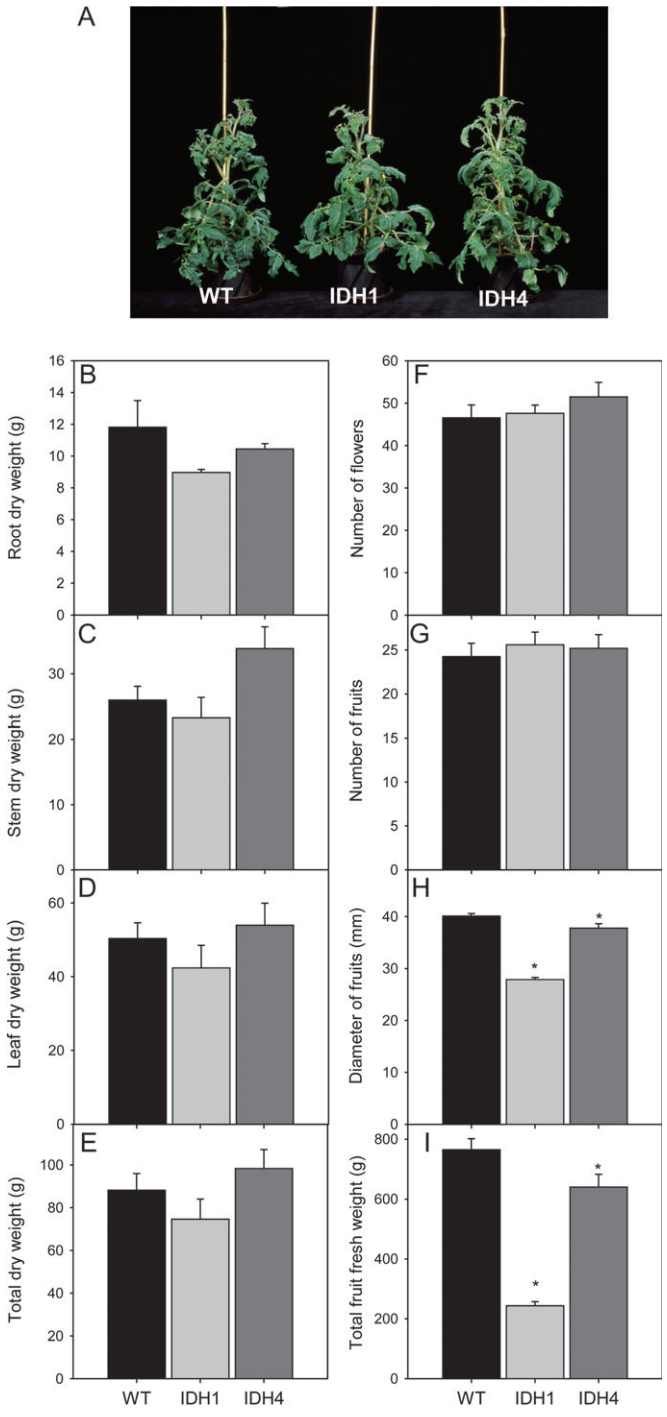

Figure 2. Growth Phenotype of IDH Transgenic Tomato Plants.

(A) Photograph showing representative plants after 4 weeks growth.

(B) Total root dry weight.

(C) Total stem dry weight.

(D) Total leaf dry weight.

(E) Total plant dry weight of 6-week-old plants.

(F) Total number of flowers and fruits **(G)**, diameter of fruits **(H)** and **(I)** total fruit fresh weight of 10-week-old plants. Values are presented as means ± SE (n = 6); an asterisk indicates values that were determined by the t-test to be significantly different ($P < 0.05$) from the wild-type.

in these parameters. For this purpose, we performed direct measurement of gas exchange under photon flux densities (PFD) that ranged from 0 to 1200 μmol m^{-2} s^{-1}. In contrast to our previous studies, we observed no major differences in either assimilation rate or dark respiration (Figure 3A). Moreover, when we measured the rate of chloroplastic electron transfer, this parameter was found to be unaltered in the transformants (Figure 3B). Surprisingly, when we closely evaluated chlorophyll fluorescence parameters, a minor and significant reduction in the PSII maximum efficiency after dark adaptation (Fv/Fm) was observed in both lines (Figure 3C). Despite that, protective non-photochemical mechanisms that dissipate excess excitation energy as heat (NPQ) were unaltered (Figure 3D).

Photosynthetic Carbon Metabolism in the Mitochondrial IDH Transformants

Analysis of the carbohydrate content of leaves from 5-week-old plants during a diurnal cycle revealed that the transformants were characterized by unchanged levels of sucrose (Figure 4A), glucose, and fructose (data not shown), but a significant reduction in the level of starch (Figure 4B).

In order to verify whether the reduction in the activity of IDH results in changes in other major pathways of primary metabolism, we used an established GC–MS protocol for metabolite profiling that allows us to quantify the relative levels of around 70 metabolites (Fernie et al., 2004). This study revealed considerable differences between the transgenics and the wild-type (Table 1). There were several notable changes in the contents of a range of amino acids. Namely, β-alanine (lines IDH1 and IDH4), glycine (line IDH1), and proline (both lines) were all significantly reduced, whilst asparagine (line IDH1) and tyramine (line IDH1) were significantly increased. In contrast, as would perhaps be expected given the presence of multiple isoforms capable of catalyzing their conversion, 2OG and isocitrate contents were unchanged in the transformants. Despite this, other TCA cycle intermediates such as malate (line IDH1), succinate (line IDH1), and pyruvate (line IDH4) were significantly reduced in the transformants. Several other interesting changes were also observed, such as the significant reduction in threonate (line IDH1), maleate (line IDH1), glycerate (both lines), citramalate (lines IDH1), and GABA (line IDH4), and the increase in saccharic acid (line IDH1).

Reduction of Mitochondrial IDH Activity Alters Nitrogen Assimilation

Given the considerable changes in amino acid metabolism, we next decided to evaluate nitrate assimilation and metabolism in leaves of the transformants. For this purpose, we analyzed by spectrophotometry the content of nitrate, total amino acids, and total insoluble protein in leaves. These studies revealed a significant increase in the level of nitrate in both lines (Figure 5A). The total amino acid levels were unaltered (Figure 5B), whilst, perhaps surprisingly, protein levels were increased in both lines (Figure 5C).

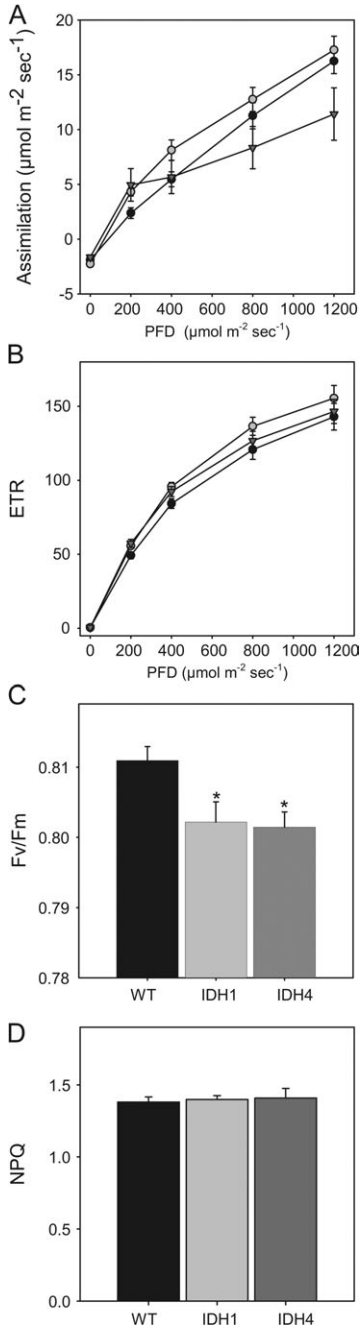

Figure 3. Physiological Parameters of IDH Transgenic Tomato Plants.

Leaf assimilation rate **(A)** and *in vivo* chlorophyll fluorescence emission, as an indicator of the relative electron transport rate (ETR) **(B)**, at photon flux density (PFD) ranging from 0 to 1200 μmol m^{-2} s^{-1}. Fv/Fm ratio as estimation of PSII maximum efficiency **(C)**. Non-photochemical quenching (NPQ) at 1200 μmol m^{-2} s^{-1} **(D)**. All measurements were performed in 4-week-old plants. Values are presented as mean ± SE (n = 6); an asterisk indicates values that were determined by the t-test to be significantly different ($P < 0.05$) from the wild-type. The lines used were: wild-type, black circles; IDH1, gray circles; IDH4, gray triangles.

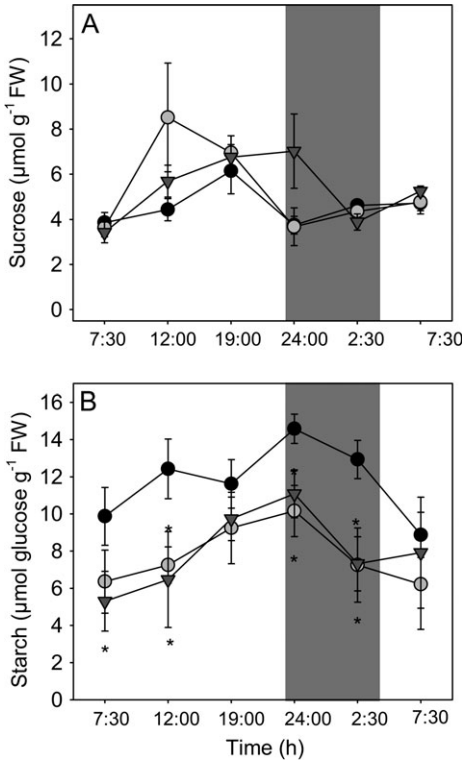

Figure 4. Diurnal Changes in Sucrose **(A)** and Starch **(B)** Content in Leaves of 6-Week-Old IDH Transgenic Tomato Plants.

At each time point, samples were taken from mature source leaves, and the data presented are mean ± SE (n = 6). Asterisk indicates values that were determined by the t-test to be significantly different ($P < 0.05$) from the wild-type. The lines used were: wild-type, black circles; IDH1, gray circles; IDH4, gray triangles. Shaded background indicates the dark period.

Pigment Contents in the Transgenic Lines

Considering the above results, we determined the levels of the photosynthetic pigments because these compounds have often been reported as important indicators of nitrogen deficiency (Gaude et al., 2007; Sienkiewicz-Porzucek et al., 2008). In accordance with our previous studies with mitochondrial citrate synthase antisense plants (Sienkiewicz-Porzucek et al., 2008), high-performance liquid chromatography (HPLC) analysis revealed a general decrease in pigment content in the transformants. Chlorophylls *a* and *b* were both significantly reduced in the transformants (both lines), as was lutein (lines IDH4), violaxanthin (significant in both lines), and zeaxanthin (line IDH4), while the levels of β-carotene, neoxanthin, and antheraxanthin were unaltered (Figure 6).

Pyridine Nucleotide Content in IDH Transgenic Plants

Since the oxidative decarboxylation of isocitrate to 2OG catalyzed by both IDH and ICDH also results in the production of reduced coenzyme NAD(P)H, it might be expected that reduction in the activity of these enzymes affects the redox balance

Table 1. Relative Metabolite Content of Fully Expanded Leaves from 5-Week-Old Plants of the IDH Transgenic Tomato Lines.

	WT	IDH1	IDH4
Amino acids			
β-alanine	1.000 ± 0.027	**0.818 ± 0.062**	**0.698 ± 0.105**
Alanine	1.000 ± 0.170	1.233 ± 0.320	0.757 ± 0.121
Arginine	1.000 ± 0.096	0.971 ± 0.021	0.918 ± 0.100
Asparagine	1.000 ± 0.047	**1.513 ± 0.116**	0.881 ± 0.075
Aspartic acid	1.000 ± 0.048	0.941 ± 0.060	0.908 ± 0.112
GABA	1.000 ± 0.036	0.924 ± 0.064	**0.832 ± 0.055**
Glutamic acid	1.000 ± 0.024	0.914 ± 0.045	0.919 ± 0.049
Glutamine	1.000 ± 0.152	0.849 ± 0.103	0.725 ± 0.119
Glycine	1.000 ± 0.063	**0.770 ± 0.026**	1.153 ± 0.064
Phenylalanine	1.000 ± 0.051	0.855 ± 0.047	1.069 ± 0.074
Proline	1.000 ± 0.065	**0.630 ± 0.047**	**0.397 ± 0.084**
Serine	1.000 ± 0.045	1.064 ± 0.046	1.058 ± 0.032
Tryptophan	1.000 ± 0.087	0.823 ± 0.107	1.021 ± 0.090
Tyramine	1.000 ± 0.083	**1.477 ± 0.168**	1.110 ± 0.080
Tyrosine	1.000 ± 0.058	1.002 ± 0.043	1.040 ± 0.092
Valine	1.000 ± 0.054	0.955 ± 0.106	1.047 ± 0.044
Isoleucine	1.000 ± 0.069	1.026 ± 0.084	1.039 ± 0.037
Organic acids			
Citric acid	1.000 ± 0.059	1.081 ± 0.121	1.056 ± 0.032
Fumaric acid	1.000 ± 0.065	0.871 ± 0.097	1.107 ± 0.145
2OG	1.000 ± 0.098	1.211 ± 0.132	1.047 ± 0.164
Glyceric acid	1.000 ± 0.063	**0.620 ± 0.122**	**0.803 ± 0.047**
Glycolic acid	1.000 ± 0.044	**0.813 ± 0.061**	1.018 ± 0.047
Isocitric acid	1.000 ± 0.051	1.138 ± 0.094	0.915 ± 0.037
Lactic acid	1.000 ± 0.060	0.842 ± 0.054	1.125 ± 0.115
Maleic acid	1.000 ± 0.074	**0.568 ± 0.083**	0.995 ± 0.083
Citramalic acid	1.000 ± 0.046	**0.613 ± 0.052**	0.884 ± 0.049
Malic acid	1.000 ± 0.022	**0.888 ± 0.026**	1.004 ± 0.014
Pyruvic acid	1.000 ± 0.067	0.980 ± 0.131	**0.740 ± 0.077**
Saccharic acid	1.000 ± 0.091	**1.557 ± 0.208**	1.149 ± 0.137
Succinic acid	1.000 ± 0.080	**0.701 ± 0.073**	0.880 ± 0.149
Threonic acid	1.000 ± 0.087	**0.568 ± 0.070**	0.859 ± 0.208
Sugars			
Fructose	1.000 ± 0.036	0.945 ± 0.011	0.952 ± 0.042
Glucose	1.000 ± 0.029	1.006 ± 0.026	1.035 ± 0.034
Maltose	1.000 ± 0.047	0.771 ± 0.091	**0.751 ± 0.071**
Sucrose	1.000 ± 0.035	0.974 ± 0.019	0.954 ± 0.031
Trehalose	1.000 ± 0.045	0.856 ± 0.058	0.959 ± 0.058

The leaf material was harvested in the middle of the light period. Data are normalized with respect to the mean response calculated for the wild-type. Values are presented as mean ± SE (n = 6). Values set in bold were determined by the t-test to be significantly different ($P < 0.05$) from the wild-type.

in the transformants. We therefore decided to assay the levels of pyridine dinucleotides in the leaves of wild-type and transformant plants. Interestingly, whilst both NADH and NADPH were significantly reduced in all transgenic lines (Figure 7A and 7B), NAD and NADP levels were unaltered in all genotypes

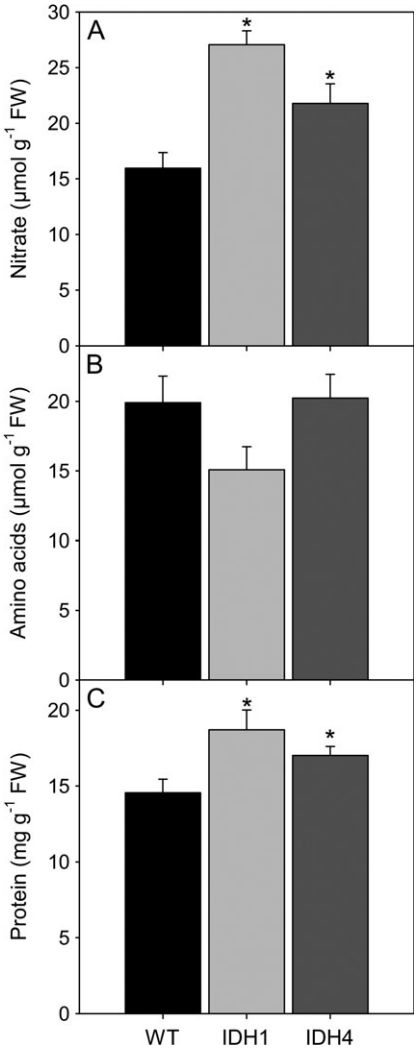

Figure 5. Nitrate, Total Amino Acids, and Protein Contents in Leaves of IDH Transgenic Tomato Plants.

The leaf material was harvested in the middle of the light period from 5-week-old plants. The data presented are mean ± SE (n = 6). Asterisk indicates values that were determined by the t-test to be significantly different ($P < 0.05$) from the wild-type.

(Figure 7C and 7D). As a result, a trend towards a decrease in the NADH/NAD and NADPH/NADP ratios was observed (Figure 7E and 7F).

Effect of Reduction of Mitochondrial IDH on the Activities of Other Enzymes of Primary Metabolism

To better understand the above-described changes in metabolites, we next analyzed the maximal activities of a wide range of key enzymes of carbon and nitrogen metabolism (Table 2). Our results suggested a reduced capacity for nitrate assimilation in the IDH lines. However, total nitrate reductase activity was not significantly altered in leaves of the transgenic plants. Interestingly, glutamate dehydrogenase (GDH) activity

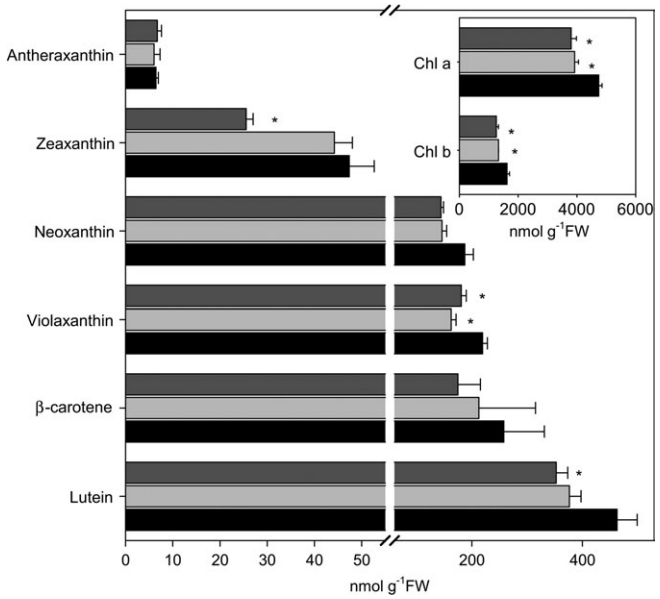

Figure 6. Pigment Content in Leaves of IDH Transgenic Tomato Plants.

Pigments were determined in 6-week-old fully expanded source leaves harvested in the middle of the day. Values presented are mean ± SE (n = 6). Asterisks indicate values that were determined by the t-test to be significantly different ($P < 0.05$) from the wild-type. The lines used were: wild-type, black bars; IDH1, light-gray bars; IDH4, gray bars.

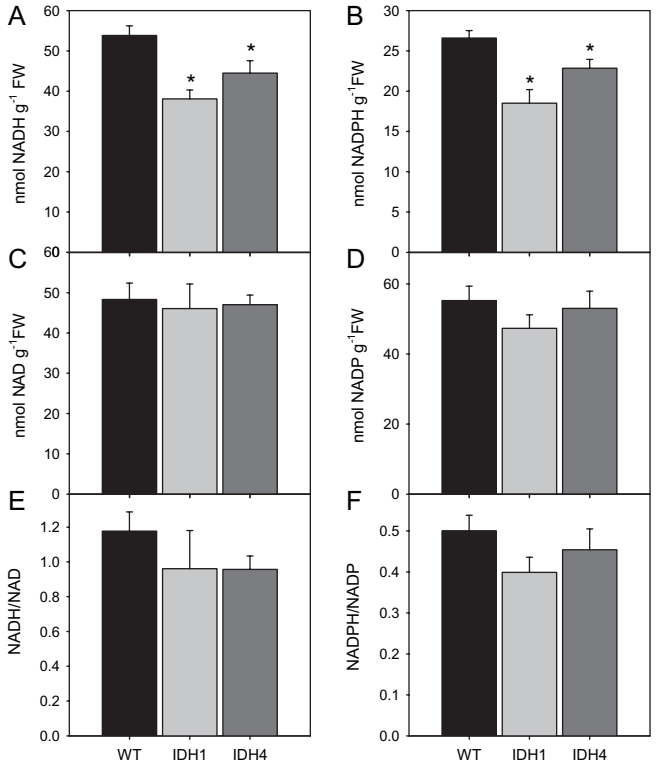

Figure 7. Pyridine Nucleotide Levels and Ratios in Leaves of IDH Transgenic Tomato Plants.

The leaf material was harvested in the middle of the light period, from 5-week-old plants. The data presented are mean ± SE (n = 6). Asterisk indicates values that were determined by the t-test to be significantly different ($P < 0.05$) from the wild-type.

significantly increased in both lines, suggesting that glutamate might be oxidized in the mitochondria in order to sustain the supply of 2OG to the TCA cycle, concomitant to the release of NH_4^+ (Robinson et al., 1991; Aubert et al., 2001). We also assayed glycerate kinase, which is a key enzyme of the photorespiratory cycle (Boldt et al., 2005). This enzyme was slightly increased in both transgenic lines, significantly so in the case of line IDH4. Considering TCA cycle enzymes, there were no significant differences in the total activities of citrate synthase, aconitase, and NAD-dependent malate dehydrogenase. However, the activity of fumarase was strongly reduced in both transformants. As described before, both transgenic lines showed lower NAD(P)H levels, reduced pigment levels, and minor reduction in the efficiency of PSII. For that reason, we expected changes in the chloroplastic redox state (Scheibe, 2004). To further test this hypothesis, we assayed both initial and maximal activities of NADP-dependent malate dehydrogenase and, from these data, calculated the activation state of the enzyme. The results revealed that both total and initial NADP–MDH activities were unaltered in the both IDH lines, thus indicating no change in the activation state of NADP–MDH.

Gene Expression Profiling

To gain a broader overview of changes occurring following the genetic perturbation introduced, we additionally evaluated the relative level of a wide range of transcripts by comparing the expression levels of wild-type and line IDH4 using TOM1 microarrays (Alba et al., 2004) and displayed this on the *Solanacea* MapMan visualization (Urbanczyk-Wochniak et al., 2006; Figure 8). This display reveals that the transformants were not characterized by massive global changes in gene expression. For this reason, we chose to make use of a feature of the MapMan, which determines the over-representation of a particular functional category by evaluating the responses of all genes in a given category compared with the overall response of all gene categories on the microarray (Usadel et al., 2005). Interestingly, few categories behaved significantly in a different manner. It was observed that genes associated with the Calvin cycle were slightly down-regulated in the transformant (Figure 8A). For example, the expression of phosphoribulokinase was approximately six-fold decreased. The second functional category that substantially changed was that grouping carbonic anhydrases, where the expression of the genes corresponding to this enzyme were up to 2.5-fold reduced in the transgenic line. When we looked at the expression of genes associated with regulation, significant changes were found in three functional categories. Genes associated with protein degradation displayed a general increase in expression; for example, the Ser/Thr specific protein phosphatase increased six-fold and 26S protease regulatory subunit VII increased 2.9-fold. Similarly, G-protein-associated transcripts

Table 2. Enzyme Activities in Leaves of IDH Transgenic Tomato Lines.

	WT	IDH1 nmol min^{-1} g^{-1} FW	IDH4
Pyruvate kinase	1108.64 ± 94.20	1022.42 ± 77.10	1151.88 ± 101.68
PEP Carboxylase	1432.68 ± 96.30	1262.82 ± 43.10	1467.59 ± 46.06
Total NADP-MDH	5464.99 ± 184.15	5468.92 ± 173.55	5888.36 ± 260.32
Initial NADP-MDH	2864.59 ± 95.03	2802.55 ± 164.71	3380.89 ± 475.97
NADP-MDH activation state *	0.53 ± 0.01	0.52 ± 0.04	0.49 ± 0.01
Citrate synthase	138.41 ± 15.18	143.88 ± 11.95	145.43 ± 13.85
Aconitase	351.34 ± 40.94	326.15 ± 77.41	359.13 ± 46.05
Fumarase	5121.71 ± 853.18	**2256.55 ± 545.91**	**2533.93 ± 592.69**
NAD-MDH	75304.24 ± 4558.54	77407.00 ± 5667.24	74292.62 ± 8425.27
NAD-GDH	226.60 ± 25.16	**332.24 ± 15.92**	**338.45 ± 40.54**
Nitrate reductase	321.05 ± 32.76	356.52 ± 38.61	409.19 ± 45.32
Glycerate kinase	1963.57 ± 135.33	2087.79 ± 120.93	**2530.41 ± 198.32**

Activities were determined in 5-week-old fully expanded source leaves harvested 6 h into the photoperiod. Data presented are mean ± SE (n = 6); values set in bold type were determined by the t-test to be significantly different ($P < 0.05$) from the wild-type. FW, fresh weight; PEP, phosphoenolpyruvate; MDH, malate dehydrogenase; GDH, glutamate dehydrogenase.
* Ratio of initial NADP–MDH activity to total NADP–MDH activity.

revealed an increase of 2.5-fold of a GTP-binding protein in the transgenic line. Moreover, increase in the transcript levels was also observed for redox regulation-associated genes, such as 2-oxoglutarate-dependent dioxygenase, which was three-fold increased in the transgenic line.

Flux Analyses

We next evaluated the rate of respiration in the transformants. For this purpose, we adopted two strategies. First, we recorded the evolution of $^{14}CO_2$ following incubation of leaf discs in positionally labeled ^{14}C-glucose molecules, and, second, we used ^{13}C pyruvate feeding to directly assess flux through the TCA cycle. In the first experiment, we incubated leaf discs taken from plants in the light and supplied these with [1-^{14}C], [2-^{14}C], [3:4-^{14}C], or [6-^{14}C] glucose over a period of 6 h. During this time, we collected the $^{14}CO_2$ evolved at hourly intervals. Carbon dioxide can be released from the C1 position by the action of enzymes that are not associated with mitochondrial respiration, but carbon dioxide evolution from the C3:4 positions of glucose cannot (ap Rees and Beevers, 1960). Thus, the ratio of carbon dioxide evolution from C1 to C3:4 positions of glucose provides an indication of the relative rate of the TCA cycle with respect to other processes of carbohydrate oxidation. When the relative $^{14}CO_2$ release of the transgenic and wild-type lines was compared for the various fed substrates, an interesting pattern emerged (Figure 9). The rate of $^{14}CO_2$ evolution was always highest in leaves incubated in [1-^{14}C] glucose; however, the absolute rate of carbon dioxide evolution from the C1 position of the transgenic lines was far in excess of that observed in the wild-type. In contrast, the release from the C3:4 positions was much lower in the transgenic line (IDH1) than in the wild-type. Thus, these data suggest that a lower proportion of carbohydrate oxidation is carried out by the TCA cycle in the transgenic lines. To evaluate whether this is indeed the case, we next evaluated the relative isotope redistribution in leaves excised from wild-type and transformant plants using a combination of feeding ^{13}C-labeled substrate to the leaf via the transpiration stream and a recently adapted GC–MS protocol that facilitates the estimation of intracellular fluxes (Roessner-Tunali et al., 2004). We supplied ^{13}C-labeled pyruvate for a period of 3 h and evaluated the redistribution of ^{13}C to TCA cycle, GABA shunt, and photorespiratory pathways (Figure 10). These studies indicated that the rate of isotope redistribution to citrate was unaltered whilst that to isocitrate and 2OG was significantly reduced in both lines, as was that to glutamate (in the case of line IDH4). Given that the GABA shunt can bypass the reaction catalyzed by succinyl–coenzyme A ligase and sustain succinate supply to the TCA cycle (Studart-Guimarães et al., 2007), we additionally quantified the label redistribution to GABA. Neither the label redistribution to GABA nor that to succinate was altered in the transformants. Interestingly, however, label redistribution was markedly reduced to malate and fumarate (significant in both lines). In contrast to that general decrease in label redistribution to TCA cycle intermediates, when looking at photorespiratory pathway intermediates, a clearly increased label redistribution was observed to glycine (significantly in line IDH4) and serine (line IDH1). Taken together, these data, and those of the respiration measurements described above, hint toward a restriction in pyruvate-derived fluxes through IDH but suggest an increase in the activity of mitochondrially located photorespiratory enzymes.

DISCUSSION

Much effort has been recently invested in the study of plant photosynthetic energy metabolism in order to better

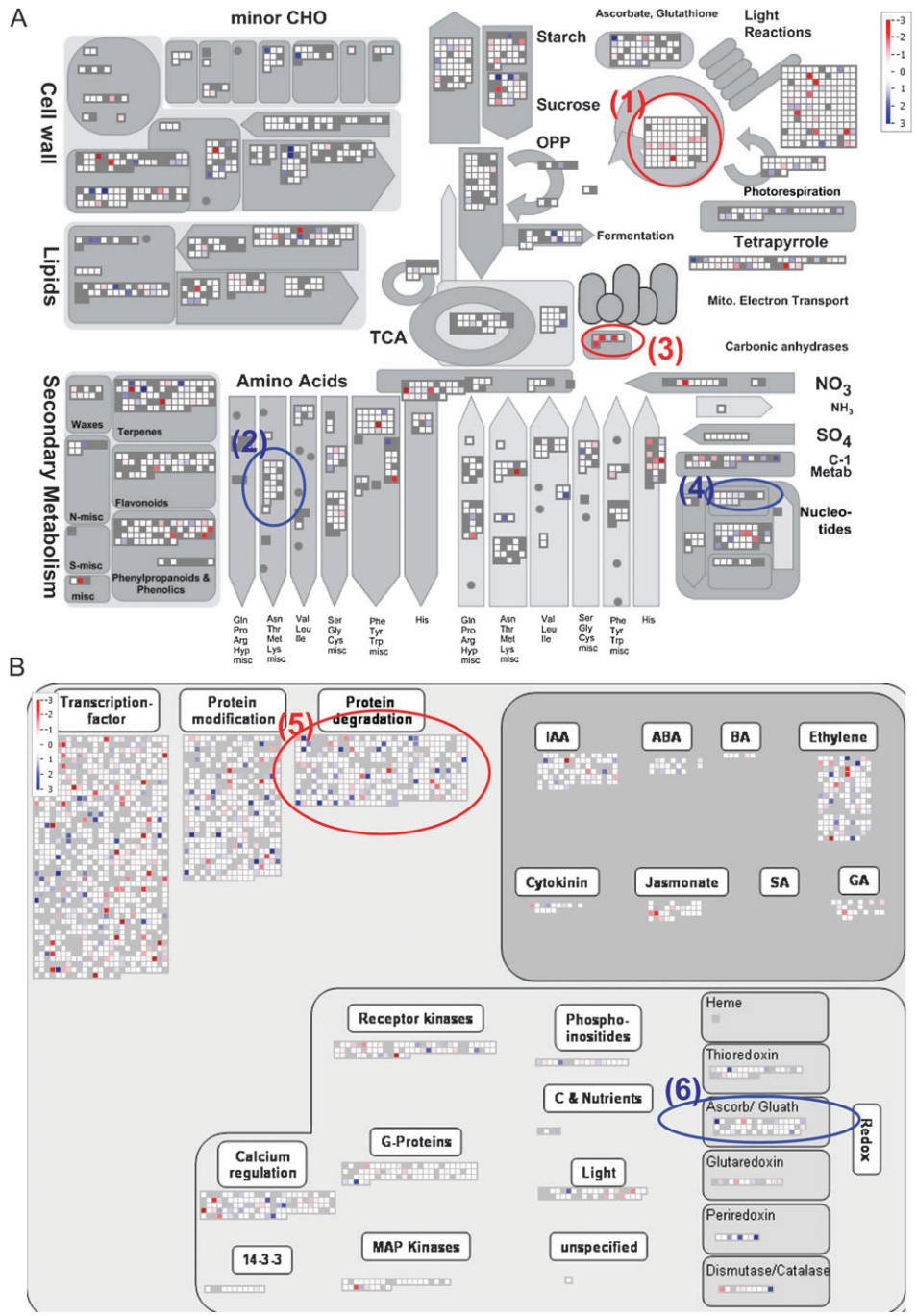

Figure 8. Differences in Transcript Levels between Leaves of IDH4 and Wild-Type for Genes Associated with Metabolism **(A)** and Regulation **(B)**.

Red and blue represent a decrease and an increase in expression, respectively, in the antisense IDH4 line with respect to the wild-type. The data represent mean values of four individual plants for each genotype. The leaf material was harvested in the middle of the light period, from 5-week-old plants. The numbers in the brackets indicate four functional categories (FC) in which the genes behave in a significantly different manner from the response of all of the genes on the array. (1) FC: photosystems and Calvin cycle; (2) FC: amino acid metabolism/synthesis of aspartate family/methionine; (3) FC: TCA/organic acids transformation/carbonic anhydrases; (4) FC: nucleotide metabolism/salvage; (5) FC: protein degradation; (6) FC: redox/ascorbate and glutathione.

understand the functional role of respiratory metabolism in the illuminated leaf. Studies in which components of the mitochondrial electron transport chain were manipulated indicate that its correct functioning is required to sustain optimal rates of photosynthesis (Igamberdiev et al., 2001; Raghavendra and Padmasree, 2003; Dutilleul et al., 2003; Bartoli et al., 2005; Sweetlove et al., 2006). However, this effect is not exclusive for components of the mitochondrial electron

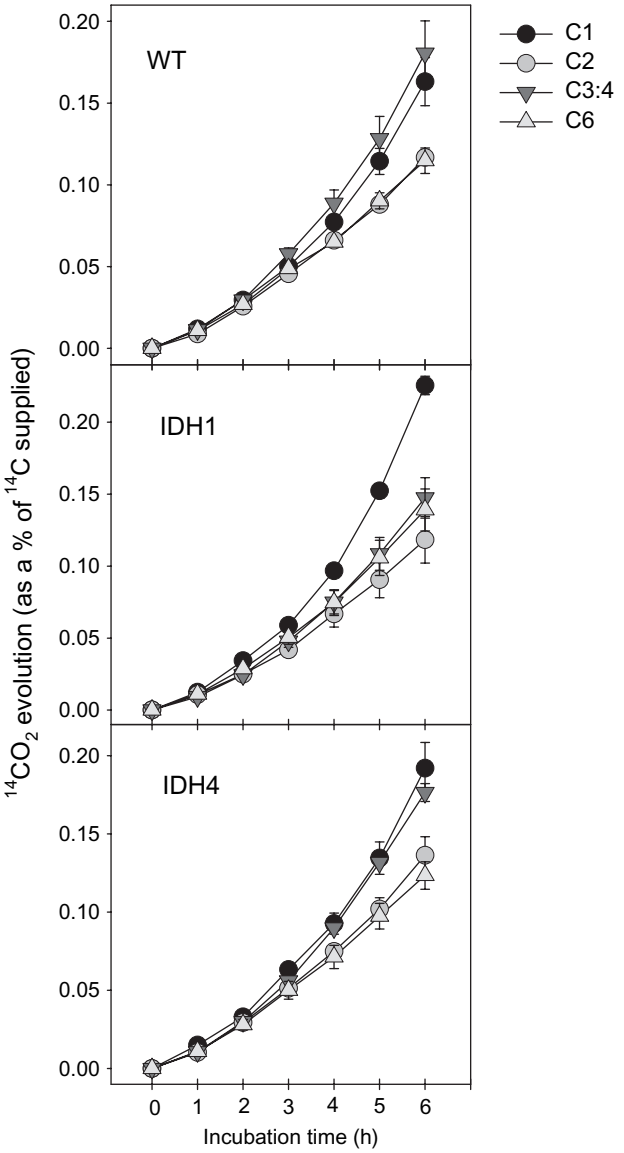

Figure 9. Respiratory Parameters in Leaves of the Antisense IDH Lines.

Evolution of $^{14}CO_2$ from isolated leaf discs in the light. The leaf discs were taken from 5-week-old plants and were incubated in 10 mM MES–KOH solution, pH 6.5, 0.3 mM glucose supplemented with 2.32 kBq mL^{-1} of [1-^{14}C], [2-^{14}C], [3:4-^{14}C], or [6-^{14}C] glucose at an irradiance of 200 μmol m^{-2} s^{-1}. The $^{14}CO_2$ liberated was captured (at hourly intervals) in a KOH trap and the amount of radiolabel released was subsequently quantified by liquid scintillation counting. The data presented are mean ± SE (n = 3).

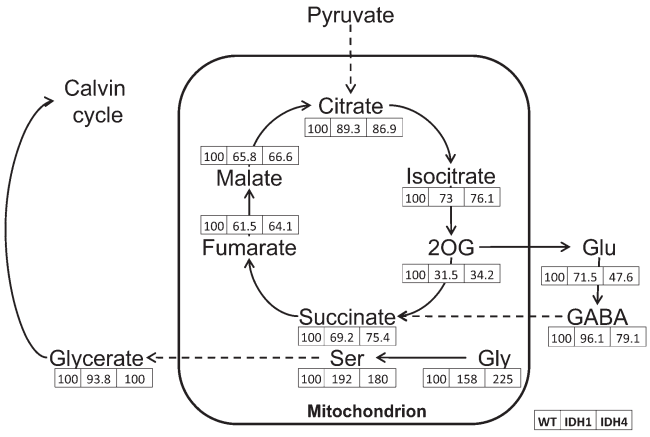

	WT	IDH1	IDH4
	μmol C_1 equivalents g^{-1}FW h^{-1}		
Citrate	1.031 ± 0.11	0.921 ± 0.051	0.896 ± 0.137
Isocitrate	0.163 ± 0.013	**0.119 ± 0.004**	**0.124 ± 0.012**
2OG	0.111 ± 0.028	**0.035 ± 0.001**	**0.038 ± 0.004**
Succinate	5.129 ± 0.846	3.551 ± 0.204	3.866 ± 0.357
Fumarate	0.039 ± 0.003	**0.024 ± 0.004**	**0.025 ± 0.005**
Malate	7.865 ± 0.976	**5.173 ± 0.179**	**5.237 ± 0.577**
Glutamate	3.425 ± 0.589	2.448 ± 0.107	**1.63 ± 0.217**
Glycine	0.04 ± 0.009	0.063 ± 0.006	**0.09 ± 0.017**
Serine	0.088 ± 0.025	**0.169 ± 0.018**	0.158 ± 0.036
Glycerate	0.032 ± 0.004	0.03 ± 0.001	0.032 ± 0.003
GABA	4.066 ± 0.612	3.906 ± 0.241	3.216 ± 0.382

Figure 10. Redistribution of Heavy Label Following Incubation of Mitochondrial IDH Transgenics and Wild-Type Leaves via the Transpiration Stream in [U-^{13}C] Pyruvate Solution. The leaf material was harvested at the beginning of the light period, from 6-week-old plants.

Values in the table represent absolute redistribution and are given as mean ± SE (n = 6). Those set in bold type were determined by the t-test to be significantly different ($P < 0.05$) from the wild-type. Values given in the metabolic schema are normalized such that the wild-type redistribution is set at 100. The genotype is as indicated in the box.

transport chain, since studies in which several TCA cycle enzymes were genetically perturbed also displayed altered photosynthetic performance. Whilst genotypes deficient in the activity of aconitase or mitochondrial malate dehydrogenase displayed an increase in the photosynthetic rate (Carrari et al., 2003; Nunes-Nesi et al., 2005), down-regulation of fumarase resulted in a repression of photosynthesis (Nunes-Nesi et al., 2007). In contrast, modulation of citrate synthase (Sienkiewicz-Porzucek et al., 2008) and succinyl-coenzyme A ligase (Studart-Guimarães et al., 2007) activities resulted in essentially unaltered photosynthetic rates, despite showing clear alterations in metabolism. Here, we extend our ongoing survey of the TCA cycle and report on the consequences of the antisense inhibition of the *Sl*IDH1 gene, which encodes an NAD-dependent, mitochondrially localized isocitrate dehydrogenase. This enzyme is believed to be a key regulatory step of the TCA cycle as well as having importance in the maintenance of the 2OG level and therefore in the regulation of nitrogen assimilation (Lancien et al., 1999; Stitt and Fernie, 2003).

Based on amino acid sequence analyses, it appears that both IDHs identified in tomato, *Sl*IDH1 and *Sl*IDH2, are highly similar to *Nt*IDHb from tobacco and, to a lesser extent, to *At*IDH1 from *Arabidopsis* (Figure 1A). These observations thus suggest that *Sl*IDH1 and 2 encode regulatory subunits of NAD-dependent IDH in tomato and that the gene encoding the catalytic subunit has yet to be identified. In this study, we characterized two transgenic lines displaying 49 and 70% reduction in

expression levels of *Sl*IDH1 (Figure 1E), which led to decreases of 28 and 44% in total NAD-dependent IDH activity, respectively (without apparent impact on NADP-dependent isocitrate dehydrogenase; Figure 1D; subsections i and ii). When compared with the residual 8% of IDH activity observed for the corresponding *Arabidopsis* knockout mutant, where the T-DNA is inserted in a gene encoding a catalytic subunit (Lemaitre et al., 2007), the antisense inhibition of *Sl*IDH1 led to only a mild reduction in the IDH activity. Interestingly, the 44% reduction in the IDH activity observed in the strongest line reduced the fruit size by 30% and fruit yield by 68%. This effect could be explained by either an alteration in fruit sink strength, caused by altered number of fruits (sink size), or a reduced competitive ability of the fruits to import assimilates (sink activity; Herbers and Sonnewald, 1998). As we show that down-regulation of mIDH did not result in an altered number of fruits per plant (Figure 2G), the latter hypothesis seems the most likely. However, we cannot rule out the impact of the genetic perturbation on fruit metabolism *per se*. Given that we use the constitutive CaMV 35S promoter in the present work, it is clear that the activity of this enzyme will be affected in both leaves and fruits. We are, therefore, unable to distinguish whether the loss of fruit yield was due to sink or source effects. Survey of the literature revealed that in tomato, both causes are possible; the increased photosynthetic rates observed in the mMDH lines were coupled to an increased fruit yield (Nunes-Nesi et al., 2005), whereas fruit-specific reduction of cell wall invertase (Zanor et al., 2009), or plastidic FBPase (Obiadalla-Ali et al., 2004), resulted in decreased fruit yield. For this reason, the future generation of plants in which IDH activity is reduced in a tissue-specific manner will be important to resolve this question.

Given the complexities in interpreting the fruit phenotype, we focused our efforts here on understanding the influence of IDH on photosynthetic metabolism. Whilst the antisense inhibition of mitochondrial IDH resulted in unaltered rates of assimilation and chloroplastic electron transport, the maximal efficiency of photosystem II (Fv/Fm) was reduced in the transformants (Figure 3). Consistent with this alteration are the changes observed in pigment content, such as the reduction in chlorophyll a and b, violaxanthin, and zeaxanthin (Figure 6). Despite only minor changes in photosynthesis, quite considerable changes were observed in metabolism. One of the most striking effects was a decrease in starch accumulation during the day (Figure 4). It is already well known that diurnal changes in starch as well as organic acids biosynthesis are synchronized to nitrate assimilation (Scheible et al., 1997, 2000). Consistent with this, down-regulation of the mIDH also led to increased nitrate contents up to 168% of the wild-type levels but unchanged total amino acid pool sizes and, surprisingly, enhanced protein levels (Figure 5). Similar, albeit more dramatic, effects on nitrate assimilation have been previously observed in mitochondrial citrate synthase-deficient tomato plants (Sienkiewicz-Porzucek et al., 2008); however, in this case, the protein content was unchanged. While the increase in protein is admittedly somewhat at odds with an impaired nitrate assimilation, the fact that the accumulation of nitrate in the transgenics is greater than that of protein suggests a mild impairment in their capacity to assimilate nitrate, albeit one which appears to be compensated by an as yet undefined mechanism.

In addition to its role in nitrate assimilation, 2OG is a key organic acid of the TCA cycle (Lancien et al., 2000; Scheible et al., 2000). Despite this fact, it is not yet clear where the major site of production of 2OG resides. This organic acid can be produced from either sugar respiration or amino acid transamination following the concerted action of isocitrate dehydrogenases, aminotransaminases, and glutamate dehydrogenases (Lancien et al., 2000). The work reported here suggests that mIDH has an important role in 2OG production. Whereas the specific reduction of the mitochondrial IDH activity, without any effect on ICDH activity, did not result in reduction of absolute 2OG levels, the label redistribution to 2OG was clearly impaired in the transformants (Figure 10). A similar reduction in the TCA cycle activity was also demonstrated in the mitochondrial citrate synthase antisense plants (Sienkiewicz-Porzucek et al., 2008). Taken together, these results support the hypothesis that mitochondrial TCA cycle enzymes contribute to the regulation of nitrogen assimilation in leaves and that a substantial portion of 2OG production occurs in the mitochondria. It has also recently been demonstrated that other mitochondrially localized proteins have a profound impact on nitrogen metabolism (Pellny et al., 2008; Dutilleul et al., 2005). In these studies, the tobacco CMS mutant, which lacks the mitochondrial gene nad7 and thus a functional complex I, was revealed to display altered carbon/nitrogen ratios and was depleted in starch and 2OG (Dutilleul et al., 2005). The deficiency in 2OG was attributed to increased citrate and malate levels and key anaplerotic enzymes, notably mitochondrial IDH. Additional evidence has been provided by addition of rotenone, a specific inhibitor of Complex I, to *Arabidopsis* cell suspension cultures (Garmier et al., 2008). This study revealed that 2OG production is rapidly reduced after application of the inhibitor and that this decrease persisted for at least 16 h. In addition, important evidence for the role of mitochondrial metabolism in the maintenance of optimal photosynthetic performance have been provided for uncoupling protein 1 (Sweetlove et al., 2006) and alternative oxidase-1A (Strodtkötter et al., 2009), which appear to have a role in photorespiration. In the present work, metabolite profiling of the mIDH antisense lines demonstrated that steady state levels of photorespiratory intermediates, namely glycolate, glycerate, and glycine, were reduced (Table 1), although there was an increased label redistribution to glycine and serine (Figure 10). These results suggest that the down-regulation of the TCA cycle activity was integrated with an up-regulation in the flux through the photorespiration pathway as part of a reprogramming to maintain either mitochondrial NADH homeostasis and/or the glutamate pool size. NADH and NADPH levels play an important role in mitochondrial respiratory metabolism

(Noctor et al., 2007) and, under many different conditions, free mitochondrial NADH levels are kept constant (Kasimova et al., 2006). The IDH-deficient plants showed reduced NADH and NADPH levels, which are known to inhibit ICDH activity; therefore, cytosolic ICDH activity is likely to be de-inhibited in the transformants (Figure 1B, subsection i) allowing the functioning of an alternative pathway involving citrate export from mitochondria to support 2OG synthesis in the cytosol (Igamberdiev and Gardeström, 2003). Alternatively, or additionally, we might expect that glutamate levels are maintained in the transgenics via increased activity of glutamate dehydrogenase (GDH; Table 2), since increasing flux through the glycine decarboxylase reaction will result in an elevated NH_4^+ level that must consequently be assimilated to avoid its toxic effects in the cell. It is conceivable that the NH_4^+ provided by photorespiration or protein degradation and 2OG provided by the cytosolic ICDH could be metabolized by cytosolic GDH that is induced under nitrogen-limiting conditions to provide glutamate and maintain nitrogen metabolism (Tercé-Laforgue et al., 2004). Evidence for such a compensatory mechanism has been provided by antisense inhibition of ferredoxin-dependent glutamine-2-oxoglutarate aminotransferase (Fd-GOGAT) tobacco plants (Ferrario-Mery et al., 2002). Thus, it provides a clear mechanism for regulation of mitochondrial and cytosolic levels of pyridine dinucleotides, isocitrate and 2OG (Igamberdiev and Gardeström, 2003).

To summarize, in this article, we have demonstrated that minor changes in activity of mitochondrial IDH in tomato leaves has dramatic metabolic consequences but these have little effect on global patterns of transcription, growth, or plant performance. Despite this fact, this study allows several important conclusions to be made. It demonstrates a clear role for mitochondrial IDH in nitrate assimilation. Furthermore, it suggests the operation of compensatory mechanisms to maintain 2OG production that underlines the importance of this metabolite for maintenance of normal cellular function. It is clear that a mild reduction in mitochondrial IDH led to a slowing-down of the TCA cycle, and, consequently, a likely reduction in the mitochondrial levels of NADH and NADPH. This metabolic shift results in an increased activity of photorespiratory enzymes of the mitochondria. This demonstrated increase in photorespiration appears to offset the shortfall in TCA cycle activity and, consequently, may buffer the effects of the metabolic shift on the phenotype of the illuminated leaf. That said, quite clear effects were observed in the fruit of these lines, marking a detailed study of the role of the enzyme in heterotrophic tissues an important area for a future research.

METHODS

Materials

Tomato (*Solanum lycopersicum*) 'Moneymaker' was obtained from Meyer Beck. Plants were handled as described in the literature (Carrari et al., 2003). All chemicals and enzymes used in this study were obtained from Roche Diagnostics with the exception of D-(1-^{14}C) and D-(6-^{14}C) glucoses, which were from Amersham International, D-(2-^{14}C) and D-(3,4-^{14}C) glucoses were from American Radiolabeled Chemicals, and ^{13}C pyruvate was from Cambridge Isotope Laboratories.

cDNA Cloning and Expression

A 734-bp fragment of the mitochondrial *Sl*IDH1 was cloned in antisense orientation between the CaMV 35S promoter and the *ocs* terminator into the vector pBINAR (Liu et al., 1999). These constructs were introduced into plants by an *Agrobacterium*-mediated transformation protocol, and plants were selected and maintained as described in the literature (Tauberger et al., 2000). Initial screening of 67 lines was carried out using a combination of total enzyme activity determinations and Northern blot. These screens allowed the selection of two lines, which were taken to the next generation. Total IDH and ICDH activity and expression of the various isoforms of IDH and ICDH were confirmed in the second harvest of these lines.

Phylogenetic Analysis

Protein sequences were retrieved from the Gen-Bank through the BLASTp algorithm using *Sl*IDH1and *Sl*ICDH1 sequence subunits as query. Sequences were aligned using the ClustalW software package (Higgins and Sharp, 1988) using default parameters. Neighbor Joining trees (Saitou and Nei, 1987) were constructed with MEGA4.1 Beta 2 software (Tamura et al., 2007). Distances were calculated using pair-wise deletion and Poisson correction for multiple hits; bootstrap values were obtained with 500 pseudo replicates.

RNA Extraction and Quantification and qRT–PCR Analysis

The RNA and qRT–PCR were determined as described in Zanor et al. (2009). Relative quantification of the target expression of IDH and ICDH genes in WT and transgenic lines was performed using the comparative Ct method. For analysis of *Sl*IDH1 transcript levels (GenBank accession no. TC163092), the following primers were used: forward 5′-CAGTGAAGCGTGTTATTGCCG-3′, reverse 5′-GACAGCATCCGTGATTTCTTGG-3′, and *Sl*ICDH1 (GenBank accession no. TC202045), forward 5′-TCCTGATGG-CAAGACCATTGA-3′, reverse 5′-TGTGCTGGTTTCACCTCCTT-TC-3′, for *Sl*ICDH3 (GenBank accession no. TC196623), forward 5′-ATGCACGAACATTCCCAGGA-3′, reverse 5′-TGGCACGATACTGATCACCAAA-3′, for *Sl*ICDH2 (GenBank accession no. TC164449), forward 5′- GAAGCAGCCCATG-GAACTGTT-3′, reverse 5′-TCCACGAGTCCAAGCAAAAATC-3′, and for *Sl*IDH2 (GenBank accession no. TC198615) forward 5′-CTTTGAGCGATACGAAGTGCG-3′, reverse 5′-GCCCTCCT-TTCAGACAAACCTT-3′. To normalize *gene* expression for differences in the efficiency of cDNA synthesis, transcript levels of the constitutively expressed elongation factor 1-α of *Solanum lycopersicum* (GenBank accession no. X14449) and ubiquitin3 (GenBank accession no. X58253) were measured using the following primers: forward 5′-ACCACGAAGCT-CTCCAGGAG-3′, reverse 5′-CATTGAACCCAACATTGTCACC-3′,

Schaarschmidt et al. (2006) for elongation factor 1-α and forward, 5′-AGGTTGATGACACTGGAAAGGTT-3′, reverse 5′-ATCGCCTCCAGCCTTGTTGTA-3′ for ubiquitin3 (Wang et al., 2008).

Microarray Analysis

Glass slides containing arrayed tomato ESTs were obtained directly from the Center for Gene Expression Profiling (CGEP) at the Boyce Thompson Institute, Cornell University, The Geneva Agricultural Experiment Station, and the US Department of Agriculture Federal Plant and Nutrition Laboratory. The tomato array contains 13 440 spots randomly selected from cDNA libraries isolated from a range of tissues, including leaf, root, fruit, and flowers, and representing a broad range of metabolic and developmental processes. Fluorescent probe preparation and microarray hybridization and data analysis were exactly as described previously (Urbanczyk-Wochniak et al., 2006). The raw expression data were processed using Robin, a graphical application for microarray analysis. Robin facilitates the usage of advanced R/BioConductor packages (i.e. limma, RankProd (Smyth, 2004; Hong et al., 2006)) by providing an easy-to-use graphical interface to the underlying R functions. After evaluation of chip quality by visual inspection of background signal intensity, signal intensity distribution per color channel and red–green signal ratios for each chip, the data were normalized within each array using print-tip group-wise loess normalization with background subtraction and between the arrays in the experiment by scaling the log2 ratios to have the same median absolute deviation. The normalized data were statistically analyzed using the linear model-based approach implemented in the limma package using the Benjamini–Hochberg method to correct *p*-values for multiple testing.

Analysis of Enzyme Activities

Enzyme extracts were prepared as described previously (Gibon et al., 2004), except that Triton-X 100 was used at a concentration of 1% and glycerol at 20%. Citrate synthase, isocitrate dehydrogenase (NAD), phosphofructokinase (ATP) fumarase, and pyruvate kinase were assayed as described in Nunes-Nesi et al. (2007). Malate dehydrogenase (NADP) was assayed as described in Scheibe and Stitt (1988). NADP-isocitrate dehydrogenase, nitrate reductase, PEPC, and GDH (NAD) were assayed as described in Gibon et al. (2004). Glycerate kinase was assayed as described in Huege et al. (2007).

Determination of Metabolite Levels

Leaf samples were taken at the time point indicated, immediately frozen in liquid nitrogen, and stored at –80°C until further analysis. Extraction was performed by rapid grinding of tissue in liquid nitrogen and immediate addition of the appropriate extraction buffer. The levels of starch, sucrose, fructose, and glucose in the leaf tissue were determined exactly as described previously (Fernie et al., 2001). The levels of all other metabolites were quantified by GC–MS exactly following the protocol described by Roessner et al. (2001) with the exception that peak identification was optimized to tomato tissues (Roessner-Tunali et al., 2003) and extended to include newly identified peaks (Kopka et al., 2005; Schauer et al., 2005). Nitrate was determined as detailed in Fritz et al. (2006). The procedure of extraction and assay of NAD, NADH, NADP, and NAPH was performed according to the method described by Gibon and Larher (1997). Photosynthetic pigments were determined exactly as described in Bender-Machado et al. (2004).

Measurements of Photosynthetic Parameters

Four to 5-week-old plants maintained at fixed irradiance of 250 μmol photons m^{-2} s^{-1} were used for gas-exchange using a Licor-6400 gas-exchange system (Li-Cor; www.licor.com/) under different light intensities (as described in the text), 400 ppm CO_2, and a leaf temperature of 25°C. Fluorescence emission measurements to estimate the actual flux of photons driving photosystem II (ETR) was performed using a leaf chamber fluorometer (Model 6400–40, Li-Cor). The ETR and NPQ were estimated as

$$\mathrm{ETR} = [(Fm' - Fs)/Fm']\, f\, I\, \alpha_{\mathrm{leaf}}$$

$$\mathrm{NPQ} = (Fm - Fm')/Fm',$$

where *Fm* is the maximal chlorophyll a fluorescence after dark adaptation, *Fm′* is the maximal chlorophyll a fluorescence during a saturating light flash, *Fs* is steady-state fluorescence, *f* is the fraction of absorbed quanta that is used by PSII, which is assumed to be 0.5 for C3 plants, *I* is the incident PFD, and α_{leaf} is leaf absorptance that is assumed to be 0.85.

Measurement of Respiratory Parameters

Dark respiration was measured using the same gas exchange system as defined above. Estimations of the TCA cycle flux on the basis of $^{14}CO_2$ evolution were carried out following incubation of isolated leaf discs in 10 mM MES–KOH (pH 6.5) containing 2.32 KBq mL^{-1} of [1-^{14}C], [2-^{14}C], [3,4-^{14}C], or [6-^{14}C]glucose. $^{14}CO_2$ evolved was trapped in KOH and quantified by liquid scintillation counting. The results were interpreted following ap Rees and Beevers (1960).

Measurement of Redistribution of Isotope

The fate of ^{13}C-labeled pyruvate was traced following feeding of leaves excised from 6-week-old plants via the petiole placed in a solution containing 10 mM MES–KOH (pH 6.5) and 10 mM [U-^{13}C] pyruvate for 3 h. Fractional enrichment of metabolite pools was determined exactly as described previously (Roessner-Tunali et al., 2004; Tieman et al., 2006) and label redistribution was calculated as described by Studart-Guimarães et al. (2007).

Statistical Analysis

The *t*-tests were performed using the algorithm embedded into Microsoft Excel (Microsoft). The term 'significant' is used in the text only when the change in question has been confirmed to be significant ($P < 0.05$).

FUNDING

This research was partially supported by the ERA-NET TRIPTOP project funded by Deutsche Forschungsgemeinschaft (DFG; A. N-N., A.R.F.) and by the Max-Planck-Gesellschaft (A.S-P, R.S.), and by the German Ministry of Education and Research within the German Plant Genome Initiative GABI (n° 0315060E; R.S.).

ACKNOWLEDGMENTS

We are indebted to Anna Zbierzak (Max-Planck-Institut für Molekulare Pflanzenphysiologie) for pigment measurements and to Beatrice Encke and Nicole Krohn for spectrophotometric assays of metabolites. In addition, we acknowledge the excellent care of the plants by Helga Kulka (Max-Planck-Institut für Molekulare Pflanzenphysiologie). No conflict of interest declared.

REFERENCES

Abiko, T., Obara, M., Ushioda, A., Hayakawa, T., Hodges, M., and Yamaya, T. (2005). Localization of NAD-isocitrate dehydrogenase and glutamate dehydrogenase in rice roots: candidates for providing carbon skeletons to NADH–glutamate synthase. Plant Cell Physiol. **46,** 1724–1734.

Alba, R., et al. (2004). ESTs, cDNA microarrays, and gene expression profiling: tools for dissecting plant physiology and development. Plant J. **39,** 697–714.

ap Rees, T., and Beevers, H. (1960). Pathways of glucose dissimilation in carrot slices. Plant Physiol. **35,** 830–838.

Araújo, W.L., Nunes-Nesi, A., Trenkamp, S., Bunik, V.I., and Fernie, A.R. (2008). Inhibition of 2-oxoglutarate dehydrogenase in potato tuber suggests the enzyme is limiting for respiration and confirms its importance in nitrogen assimilation. Plant Physiol. **148,** 1782–1796.

Aubert, S., Bligny, R., Douce, R., Gout, E., Ratcliffe, R.G., and Roberts, J.K.M. (2001). Contribution of glutamate dehydrogenase to mitochondrial glutamate metabolism studied by ^{13}C and ^{31}P nuclear magnetic resonance. J. Exp. Bot. **52,** 37–45.

Bartoli, C.G., Gomez, F., Gergoff, G., Guiamet, J.J., and Puntarulo, S. (2005). Up-regulation of the mitochondrial alternative oxidase pathway enhances photosynthetic electron transport under drought conditions. J. Exp. Bot. **56,** 1269–1276.

Bender-Machado, L., et al. (2004). Expression of a yeast acetyl CoA hydrolase in the mitochondrion of tobacco plants inhibits growth and restricts photosynthesis. Plant Mol. Biol. **55,** 645–662.

Bläsing, O., Gibon, Y., Günther, M., Höhne, M., Osuna, D., Thimm, T., Scheible, W.-R., Morcuende, R., and Stitt, M. (2005). Sugars and circadian regulation make major contributions to the global regulation of diurnal gene expression in *Arabidopsis*. Plant Cell. **17,** 3257–3281.

Boldt, R., Edner, C., Kolukisaoglu, Ü, Hagemann, M., Weckwerth, W., Wienkoop, S., Morgenthal, K., and Bauwe, H. (2005). D-glycerate 3-kinase, the last unknown enzyme in the photorespiratory cycle in *Arabidopsis*, belongs to a novel kinase family. Plant Cell. **17,** 2413–2420.

Carrari, F., Nunes-Nesi, A., Gibon, Y., Lytovchenko, A., Ehlers-Loureiro, M., and Fernie, A.R. (2003). Reduced expression of aconitase results in an enhanced rate of photosynthesis and marked shifts in carbon partitioning in illuminated leaves of wild species tomato. Plant Physiol. **133,** 1322–1335.

Chen, R. (1998). Plant NADP-dependent isocitrate dehydrogenases are predominantly localized in the cytosol. Planta. **207,** 280–285.

Chen, R.D., and Gadal, P. (1990). Do the mitochondria provide the 2-oxoglutarate needed for glutamate synthesis in higher plant chloroplasts? Plant Physiol. Biochem. **28,** 141–145.

Corpas, F.J., Barroso, J.B., Sandalio, L.M., Palma, J.M., Lupianez, J.A., and del Rio, L.A. (1999). Peroxisomal NADP-dependent isocitrate dehydrogenase: characterization and activity regulation during natural senescence. Plant Physiol. **121,** 921–928.

Czechowski, T., Bari, R.P., Stitt, M., Scheible, W.R., and Udvardi, M.K. (2004). Real-time RT-sensitivity reveals novel root- and shoot-specific genes. Plant J. **38,** 366–379.

Dutilleul, C., Driscoll, S., Cornic, G., De Paepe, R., Foyer, C.H., and Noctor, G. (2003). Functional mitochondrial complex I is required for optimal photosynthetic performance in photorespiratory conditions and during transients. Plant Physiol. **131,** 264–275.

Dutilleul, C., Lelarge, C., Prioul, J.L., De Paepe, R., Foyer, C.H., and Noctor, G. (2005). Mitochondria-driven changes in leaf NAD status exert a crucial influence on the control of nitrate assimilation and the integration of carbon and nitrogen metabolism. Plant Physiol. **139,** 64–78.

Fernie, A.R., Carrari, F., and Sweetlove, L.J. (2004). Respiratory metabolism: glycolysis, the TCA cycle and mitochondrial electron transport chain. Curr. Opin. Plant Biol. **7,** 254–261.

Fernie, A.R., Roscher, A., Ratcliffe, R.G., and Kruger, N.J. (2001). Fructose 2,6-bisphosphate activates pyrophosphate: fructose 6 phosphate 1-phosphotransferase and increases triose phosphate to hexose phosphate cycling in heterotrophic cells. Planta. **212,** 250–263.

Ferrario-Mery, S., Hodges, M., Hirel, B., and Foyer, C.H. (2002). Photorespiration-dependent increases in phosphoenolpyruvate carboxylase, isocitrate dehydrogenase and glutamate dehydrogenase in transformed tobacco plants deficient in ferredoxin-dependent glutamine-a-ketoglutarate aminotransferase. Planta. **214,** 877–886.

Fieuw, S., Müller-Röber, B., Gálvez, S., and Willmitzer, L. (1995). Cloning and expression analysis of the cytosolic $NADP^+$-dependent isocitrate dehydrogenase from potato. Plant Physiol. **107,** 905–913.

Fritz, C., Palacios-Rojas, N., Feil, R., and Stitt, M. (2006). Regulation of secondary metabolism by the carbon-nitrogen status in tobacco: nitrate inhibits large sectors of phenylpropanoid metabolism. Plant J. **46,** 533–548.

Gallardo, F., Gálvez, S., Gadal, P., and Canovas, F.M. (1995). Changes in NADP+-linked isocitrate dehydrogenase during tomato fruit ripening. Planta. **196,** 148–154.

Gálvez, S., Bismuth, E., Sarda, C., and Gadal, P. (1994). Purification and characterization of chloroplast NADP-isocitrate dehydrogenase from mixotrophic tobacco cells: comparison with the cytosolic isoenzyme. Plant Physiol. **105,** 593–600.

Gálvez, S., Hodges, M., Decottignies, P., Bismuth, E., Lancien, M., Sangwan, R.S., Dubois, F., LeMaréchal, P., Cretin, C., and Gadal, P. (1996). Identification of a tobacco cDNA encoding

a cytosolic NADP-isocitrate dehydrogenase. Plant Mol. Biol. **30,** 307–320.

Gálvez, S., Lancien, M., and Hodges, M. (1999). Are isocitrate dehydrogenases and 2-oxoglutarate involved in the regulation of glutamate synthesis? Trends Plant Sci. **4,** 484–490.

Gálvez, S., Roche, O., Bismuth, E., Brown, S., Gadal, P., and Hodges, M. (1998). Mitochondrial localization of a NADP-dependent isocitrate dehydrogenase isoenzyme by using the green fluorescent protein as a marker. Proc. Natl Acad. Sci. U S A. **95,** 7813–7818.

Garmier, M., Carroll, A.J., Delannoy, E., Vallet, C., Day, D.A., Small, I.D., and Millar, A.H. (2008). Complex I dysfunction redirects cellular and mitochondrial metabolism in *Arabidopsis*. Plant Physiol. **148,** 1324–1341.

Gaude, N., Brehelin, C., Tischendorf, G., Kessler, F., and Dormann, P. (2007). Nitrogen deficiency in *Arabidopsis* affects galactolipid composition and gene expression and results in accumulation of fatty acid phytyl esters. Plant J. **49,** 729–739.

Gibon, Y., and Larher, F. (1997). Cycling assay for nicotinamide adenine dinucleotides: NaCl precipitation and ethanol solubilization of the reduced tetrazolium. Anal. Biochem. **251,** 153–157.

Gibon, Y., Blaesing, O.E., Hannemann, J., Carrillo, P., Hohne, M., Hendriks, J.H., Palacios, N., Cross, J., Selbig, J., and Stitt, M. (2004). A Robot-based platform to measure multiple enzyme activities in *Arabidopsis* using a set of cycling assays: comparison of changes of enzyme activities and transcript levels during diurnal cycles and in prolonged darkness. Plant Cell. **16,** 3304–3325.

Gray, G.R., Villarimo, A.R., Whitehead, C.L., and McIntosh, L. (2004). Transgenic tobacco (*Nicotiana tabacum* L.) plants with increased expression levels of mitochondrial NADP+-dependent isocitrate dehydrogenase: evidence implicating this enzyme in the redox activation of the alternative oxidase. Plant Cell Physiol. **45,** 1413–1425.

Herbers, K., and Sonnewald, U. (1998). Molecular determinants of sink strength. Curr. Opin. Plant Biol. **1,** 207–216.

Higgins, D.G., and Sharp, P.M. (1988). CLUSTAL: a package for performing multiple sequence alignment on a microcomputer. Gene. **73,** 237–244.

Hodges, M. (2002). Enzyme redundancy and the importance of 2-oxoglutarate in plant ammonium assimilation. J. Exp. Bot. **53,** 905–916.

Hodges, M., Fleish, V., Gálvez, S., and Bismuth, E. (2003). Higher plant NADP dependent isocitrate dehydrogenases, ammonium assimilation and NADPH production. Plant Physiol. Biochem. **41,** 577–585.

Hong, F., Breitling, R., McEntee, C.W., Wittner, B.S., Nemhauser, J.L., and Chory, J. (2006). RankProd: a bioconductor package for detecting differentially expressed genes in meta-analysis. Bioinformatics. **22,** 2825–2827.

Huege, J., Sulpice, R., Gibon, Y., Lisec, J., Koehl, K., and Kopka, J. (2007). GC–EI–TOF–MS analysis of *in vivo* carbon-partitioning into soluble metabolite pools of higher plants by monitoring isotope dilution after (CO_2)-C-13 labelling. Phytochemistry. **68,** 2258–2272.

Igamberdiev, A.U., and Gardeström, P. (2003). Regulation of NAD- and NADP-dependent isocitrate dehydrogenases by reduction levels of pyridine nucleotides in mitochondria and cytosol of pea leaves. Biochim. Biophys. Acta. **1606,** 117–125.

Igamberdiev, A.U., Romanowska, E., and Gardeström, P. (2001). Photorespiratory flux and mitochondrial contribution to energy and redox balance of barley leaf protoplasts in the light and during light-dark transitions. J. Plant Physiol. **158,** 1325–1332.

Jo, S.H., et al. (2001). Control of mitochondrial redox balance and cellular defense against oxidative damage by mitochondrial NADP+-dependent isocitrate dehydrogenase. J. Biol. Chem. **276,** 16168–16176.

Karimi, M., Inzé, D., and Depicker, A. (2002). GATEWAY vectors for Agrobacterium-mediated plant transformation. Trends Plant Sci. **7,** 193–195.

Kasimova, M.A., Grigiene, J., Krab, K., Hagedorn, P.H., Flyvbjerg, H., Andersen, P.E., and Møller, I.M. (2006). The free NADH concentration is kept constant in plant mitochondria under different metabolic conditions. Plant Cell. **18,** 688–698.

Kopka, J., et al. (2005). GMD@CSB.DB: the Golm Metabolome Database. Bioinformatics. **21,** 1635–1638.

Kruse, A., Fieuw, S., Heineke, D., and Müller-Röber, B. (1998). Antisense inhibition of cytosolic NADP-dependent isocitrate dehydrogenase in transgenic potato plants. Planta. **205,** 82–91.

Lancien, M., Ferrario-Mery, S., Roux, V., Bismuth, E., Masclaux, C., Hirel, B., Gadal, P., and Hodges, M. (1999). Simultaneous expression of NAD-dependent isocitrate dehydrogenase and other Krebs cycle genes after nitrate resupply to short-term nitrogen-starved tobacco. Plant Physiol. **120,** 717–725.

Lancien, M., Gadal, P., and Hodges, M. (1998). Molecular characterization of higher plant NAD-dependent isocitrate dehydrogenase: evidence for a heteromeric structure by the complementation of yeast mutants. Plant J. **16,** 325–333.

Lancien, M., Gadal, P., and Hodges, M. (2000). Enzyme redundancy and the importance of 2-oxoglutarate in higher plant ammonium assimilation. Plant Physiol. **123,** 817–824.

Landschütze, V., Willmitzer, L., and Müller-Röber, B. (1995). Inhibition of flower formation by antisense repression of mitochondrial citrate synthase in transgenic potato plants leads to specific disintegration of the ovary tissues of flowers. EMBO J. **14,** 660–666.

Lemaitre, T., and Hodges, M. (2006). Expression analysis of *Arabidopsis thaliana* NAD-dependent isocitrate dehydrogenase genes shows the presence of a functional subunit that is mainly expressed in the pollen and absent from vegetative organs. Plant Cell Physiol. **47,** 634–643.

Lemaitre, T., Urbanczyk-Wochniak, E., Flesch, V., Bismuth, E., Fernie, A.R., and Hodges, M. (2007). NAD-dependent isocitrate dehydrogenase mutants of *Arabidopsis* suggest the enzyme is not limiting for nitrogen assimilation. Plant Physiol. **144,** 1546–1558.

Liu, X.J., Prat, S., Willmitzer, L., and Frommer, W.B. (1999). *Cis*-regulatory elements directing tuber specific and sucrose inducible expression of a chimeric class I patatin promoter–GUS gene fusion. Mol. Gen. Genet. **223,** 101–106.

Møller, I.M., and Rasmusson, A.G. (1998). The role of NADP in the mitochondrial matrix. Trends Plant Sci. **3,** 21–27.

Noctor, G., De Paepe, R., and Foyer, C.H. (2007). Mitochondrial redox biology and homeostasis in plants. Trends Plant Sci. **12,** 125–134.

Nunes-Nesi, A., Carrari, F., Gibon, Y., Sulpice, R., Lytovchenko, A., Fisahn, J., Graham, J., Ratcliffe, R.G., Sweetlove, L.J., and Fernie, A.R. (2007). Deficiency of mitochondrial fumarase activity in tomato plants impairs photosynthesis via an effect on stomatal function. Plant J. **50,** 1093–1106.

Nunes-Nesi, A., Carrari, F., Lytovchenko, A., Smith, A.M.O., Ehlers-Loureiro, M., Ratcliffe, R.G., Sweetlove, L.J., and Fernie, A.R. (2005). Enhanced photosynthetic performance and growth as a consequence of decreasing mitochondrial malate dehydrogenase activity in transgenic tomato plants. Plant Physiol. **137,** 611–622.

Nunes-Nesi, A., Sulpice, R., Gibon, Y., and Fernie, A.R. (2008). The enigmatic contribution of mitochondrial function in photosynthesis. J. Exp. Bot. **59,** 1675–1684.

Obiadalla-Ali, H., Fernie, A.R., Lytovchenko, A., Kossmann, J., and Lloyd, J.R. (2004). Inhibition of chloroplastic fructose 1,6-bisphosphatase in tomato fruits leads to surprisingly small changes in carbohydrate metabolism and decreases fruit size. Planta. **219,** 533–540.

Palomo, J., Gallardo, F., Suarez, M.F., and Canovas, F.M. (1998). Purification and characterization of $NADP^+$-linked isocitrate dehydrogenase from Scots pine. Plant Physiol. **118,** 617–626.

Pellny, T.K., et al. (2008). Mitochondrial respiratory pathways modulate nitrate sensing and nitrogen-dependent regulation of plant architecture in *Nicotiana sylvestris*. Plant J. **54,** 976–992.

Raghavendra, A.S., and Padmasree, K. (2003). Beneficial interactions of mitochondrial metabolism with photosynthetic carbon assimilation. Trends Plant Sci. **8,** 546–553.

Robinson, S.A., Slade, A.P., Fox, G.G., Phillips, R., Ratcliffe, R.G., and Stewart, G.R. (1991). The role of glutamate dehydrogenase in plant nitrogen metabolism. Plant Physiol. **95,** 509–516.

Roessner, U., Luedemann, A., Brust, D., Fiehn, O., Linke, T., Willmitzer, L., and Fernie, A.R. (2001). Metabolic profiling allows comprehensive phenotyping of genetically or environmentally modified plant systems. Plant Cell. **13,** 11–29.

Roessner-Tunali, U., Hegemann, B., Lytovchenko, A., Carrari, F., Bruedigam, C., Granot, D., and Fernie, A.R. (2003). Metabolic profiling of transgenic tomato plants overexpressing hexokinase reveals that the influence of hexose phosphorylation diminishes during fruit development. Plant Physiol. **133,** 84–99.

Roessner-Tunali, U., Liu, J., Leisse, A., Balbo, I., Perez-Melis, A., Willmitzer, L., and Fernie, A.R. (2004). Kinetics of labelling of organic and amino acids in potato tubers by gas chromatography-mass spectrometry following incubation in C-14 labelled isotopes. Plant J. **39,** 668–679.

Saitou, N., and Nei, M. (1987). The neighbor-joining method: a new method for reconstructing phylogenetic trees. Mol. Biol. Evol. **4,** 406–425.

Schaarschmidt, S., Roitsch, T., and Hause, B. (2006). Arbuscular mycorrhiza induces gene expression of the apoplastic invertase LIN6 in tomato (*Lycopersicon esculentum*) roots. J. Exp. Bot. **57,** 4015–4023.

Schauer, N., et al. (2005). GC–MS libraries for the rapid identification of metabolites in complex biological samples. FEBS Lett. **579,** 1332–1337.

Scheibe, R. (2004). Malate valves to balance cellular energy balance. Physiol. Plant. **120,** 21–26.

Scheibe, R., and Stitt, M. (1988). Comparison of NADP-malate dehydrogenase activation QA reduction and O_2 evolution in spinach leaves. Plant Physiol. Biochem. **26,** 473–481.

Scheible, W.R., Gonzalez-Fontes, A., Lauerer, M., Müller-Röber, B., Caboche, M., and Stitt, M. (1997). Nitrate acts as a signal to induce organic acid metabolism and represses starch metabolism in tobacco. Plant Cell. **9,** 783–798.

Scheible, W.R., Krapp, A., and Stitt, M. (2000). Reciprocal diurnal changes of phosphoenolpyruvate and NADP-isocitrate dehydrogenase expression regulate organic acid metabolism during nitrate assimilation in tobacco leaves. Plant Cell Environ. **23,** 1155–1167.

Schneidereit, J., Häusler, R.E., Fiene, G., Kaiser, W.M., and Weber, A.P.M. (2006). Antisense repression reveals a crucial role of the plastidic 2-oxoglutarate/malate translocator DiT1 at the interface between carbon and nitrogen metabolism. Plant J. **45,** 206–224.

Siedow, J.N., and Day, D.A. (2000). Respiration and photorespiration. In Biochemistry and Molecular Biology of Plants, Buchanan B. Gruissem W. and Jones R., eds (Rockville, MD: American Society of Plant Physiologists), pp. 676–728.

Sienkiewicz-Porzucek, A., Nunes-Nesi, A., Sulpice, R., Lisec, J., Centeno, D.C., Carillo, P., Leisse, A., Urbanczyk-Wochniak, E., and Fernie, A.R. (2008). Mild reductions in mitochondrial citrate synthase activity result in a compromised nitrate assimilation and reduced leaf pigmentation but have no effect on photosynthetic performance or growth. Plant Physiol. **147,** 115–127.

Smyth, G.K. (2004). Linear models and empirical bayes methods for assessing differential expression in microarray experiments. Stat. Appl. Genet. Mol. Biol. **3,** 1–29.

Stitt, M., and Fernie, A.R. (2003). From measurement of metabolites to metabolomics. An 'on the fly' perspective illustrated by recent studies of carbon–nitrogen interactions. Curr. Opin. Biotechnol. **14,** 136–144.

Strodtkötter, I., et al. (2009). Induction of the AOX1D isoform of alternative oxidase in *A-thaliana* T-DNA insertion lines lacking isoform AOX1A is insufficient to optimize photosynthesis when treated with antimycin A. Mol. Plant. **2,** 284–297.

Studart-Guimarães, C., Fait, A., Nunes-Nesi, A., Carrari, F., Usadel, B., and Fernie, A.R. (2007). Reduced expression of succinyl CoA ligase can be compensated for by an upregulation of the γ-amino-butyrate (GABA) shunt in illuminated tomato leaves. Plant Physiol. **145,** 626–639.

Sweetlove, L.J., Fait, A., Nunes-Nesi, A., Williams, T., and Fernie, A.R. (2007). The mitochondrion: an integration point in cellular metabolism and signalling. Crit. Rev. Plant Sci. **26,** 17–43.

Sweetlove, L.J., Lytovchenko, A., Morgan, M., Nunes-Nesi, A., Taylor, N.L., Baxter, C.J., Eickmeier, I., and Fernie, A.R. (2006). Mitochondrial uncoupling protein is required for efficient photosynthesis. Proc. Natl Acad. Sci. U S A. **103,** 19587–19592.

Tamura, K., Dudley, J., Nei, M., and Kumar, S. (2007). MEGA4: Molecular Evolutionary Genetics Analysis (MEGA) software version 4.0. Mol. Biol. Evol. **24,** 1596–1599.

Tauberger, E., Fernie, A.R., Emmermann, M., Renz, A., Kossmann, J., Willmitzer, L., and Trethewey, R.N. (2000). Antisense inhibition

of plastidial phosphoglucomutase provides compelling evidence that potato tuber amyloplasts import carbon from the cytosol in the form of glucose 6-phosphate. Plant J. **23,** 43–53.

Tercé-Laforgue, T., Dubois, F., Ferrario-Mery, S., Pou de Crecenzo, M.A., Sangwan, R., and Hirel, B. (2004). Glutamate dehydrogenase of tobacco is mainly induced in the cytosol of phloem companion cells when ammonia is provided either externally or released during photorespiration. Plant Physiol. **136,** 4308–4317.

Tieman, D., Taylor, M., Schauer, N., Fernie, A.R., Hanson, A.D., and Klee, H.J. (2006). Tomato aromatic amino acid decarboxylases participate in synthesis of the flavor volatiles 2-phenylethanol and 2-phenylacetaldehyde. Proc. Natl Acad. Sci. U S A. **103,** 8287–8292.

Urbanczyk-Wochniak, E., Baxter, C., Kolbe, A., Kopka, J., Sweetlove, L.J., and Fernie, A.R. (2005). Profiling of diurnal patterns of metabolite and transcript abundance in potato (*Solanum tuberosum*) leaves. Planta. **221,** 891–903.

Urbanczyk-Wochniak, E., et al. (2006). Conversion of MapMan to allow the analysis of transcript data from Solanaceous species: effects of genetic and environmental alterations in energy metabolism in the leaf. Plant Mol. Biol. **60,** 773–792.

Usadel, B., Nagel, A., Thimm, O., Redestig, H., Blaesing, O.E., Palacios-Rojas, N., Selbig, J., Hannemann, J., Piques, M.C., and Steinhauser, D. (2005). Extension of the visualization tool MapMan to allow statistical analysis of arrays, display of corresponding genes, and comparison with known responses. Plant Physiol. **138,** 1195–1204.

Van der Hoeven, R., Ronning, C., Giovannoni, J., Martin, G., and Tanksley, S. (2003). Deductions about the number, organization and evolution of genes in the tomato genome based on analysis of a large expressed sequence tag collection and selective genomic sequencing. Plant Cell. **14,** 1441–1456.

Van der Merwe, M.J., Osorio, S., Moritz, T., Nunes-Nesi, A., and Fernie, A.R. (2009). Decreased mitochondrial activities of malate dehydrogenase and fumarase in tomato lead to altered root growth and architecture via diverse mechanisms. Plant Physiol. **149,** 653–669.

Wang, S., Liu, J., Feng, Y., Niu, X., Giovannoni, J., and Liu, Y. (2008). Altered plastid levels and potential for improved fruit nutrient content by downregulation of the tomato DDB1-interacting protein CUL4. Plant J. **55,** 89–103.

Zanor, M.I., et al. (2009). RNA interference of LIN5 in *Solanum lycopersicum* confirms its role in controlling Brix content, uncovers the influence of sugars on the levels of fruit hormones and demonstrates the importance of sucrose cleavage for normal fruit development and fertility. Plant Physiol. **150,** 1204–1218.